
# BRNO UNIVERSITY OF TECHNOLOGY
VYSOKÉ UČENÍ TECHNICKÉ V BRNĚ

## FACULTY OF MECHANICAL ENGINEERING
FAKULTA STROJNÍHO INŽENÝRSTVÍ

## INSTITUTE OF MATHEMATICS
ÚSTAV MATEMATIKY


# FOLLOWING OF MULTIPLE OBJECT MOVEMENT BY MEANS OF CROSS CORRELATION
MONITOROVÁNÍ POHYBU VÍCE OBJEKTŮ UŽITÍM KŘÍŽOVÉ KORELACE

MASTER'S THESIS
DIPLOMOVÁ PRÁCE


AUTHOR
AUTOR PRÁCE

Bc. Eliška Málková

SUPERVISOR
VEDOUCÍ PRÁCE

prof. RNDr. Miloslav Druckmüller, CSc.



BRNO 2019

VYSOKÉ UČENÍ TECHNICKÉ V BRNĚ
FAKULTA STROJNÍHO INŽENÝRSTVÍ

# Zadání diplomové práce

| | |
|---|---|
| Ústav: | Ústav matematiky |
| Studentka: | **Bc. Eliška Málková** |
| Studijní program: | Aplikované vědy v inženýrství |
| Studijní obor: | Matematické inženýrství |
| Vedoucí práce: | **prof. RNDr. Miloslav Druckmüller, CSc.** |
| Akademický rok: | 2018/19 |

Ředitel ústavu Vám v souladu se zákonem č.111/1998 o vysokých školách a se Studijním a zkušebním řádem VUT v Brně určuje následující téma diplomové práce:

## Monitorování pohybu více objektů užitím křížové korelace

**Stručná charakteristika problematiky úkolu:**

Úkolem práce je popsat a implementovat metodu monitorování translačního pohybu dvou a více objektů v digitálním obraze.

**Cíle diplomové práce:**

Popsat metodu analýzy translačního pohybu užitím křížové korelace, zobecnit ji na dva a více objektů a metodu implementovat na počítači.

**Seznam doporučené literatury:**

GOSHTASBY, A. Ardeshir. Image Registration: Principles: Tools and Methods. 1. London: Springer, 2012. ISBN 978-1-4471-2457-3.

DRUCKMÜLLEROVÁ, Hana. Phase correlation: The mathematical background and application to image registration. 1. Saarbrücken: LAMBERT Academic Publishing, 2011. ISBN 3846550914.

Termín odevzdání diplomové práce je stanoven časovým plánem akademického roku 2018/19

V Brně, dne

L. S.

| | |
|---|---|
| prof. RNDr. Josef Šlapal, CSc.<br>ředitel ústavu | doc. Ing. Jaroslav Katolický, Ph.D.<br>děkan fakulty |

**Abstrakt**
Tato práce popisuje metodu analýzy translačního pohybu užitím křížové korelace. Ukazujeme, jakým způsobem se chová funkce křížové korelace obrazů s navzájem posunutými objekty, a jak nám to umožňuje nacházet jejich vektory posunu. Pro následnou implementaci je nalezena efektivní metoda pro hledání pouze požadovaného počtu lokálních maxim funkce.

**Abstract**
This thesis describes the method of following the multiple objects movement by means of cross correlation. We are showing the form of cross-correlation function of functions with mutually shifted objects and how it leads to search of their shift vectors. For the further implementation, there is introduced the effective method for search of required count of function's local maxima.

**klíčová slova**
Fourierova transformace, posunuté funkce, posunuté objekty ve funkci konvoluce, funkce křížové korelace, funkce fázové korelace, sub-pixelová přesnost, posuny více objektů

**keywords**
Fourier transform, shifted function, shifted objects in function, convolution, cross-correlation function, phase-correlation function, sub-pixel precision, multiple object shifts

MÁLKOVÁ, Eliška. *Monitorování pohybu více objektů užitím křížové korelace.* Brno, 2019. Dostupné také z: `https://www.vutbr.cz/studenti/zav-prace/detail/115420`. Diplomová práce. Vysoké učení technické v Brně, Fakulta strojního inženýrství, Ústav matematiky. Vedoucí práce Miloslav Druckmüller.

# Rozšířený abstrakt

Monitorování pohybu více objektů v obraze je proces použitelný například ke studiu buněčného transportu mikroskopických částic, či k popisu pohybu a sociálního chování živočišných skupin. Dále může být použit i k pozorování vzájemných pohybů vesmírných těles, nebo k analýze záznamů z dopravních kamer.

Monitorování pohybu více objektů v obraze užitím křížové korelace je zobecněním metody pro hledání translace posunutých obrazů. Toto je totiž pouze monitorování pohybu jediného objektu, kterým je celý obraz. Standartní registrace obrazů je proces hledání podobnosti mezi obrazy, to zahrnuje hledání jejich posunů, rotace a změny měřítka. Bereme-li v úvahu obraz složený z více objektů, hledáme pouze posuny těchto objektů. Rozeznání rotace a změny měřítka by totiž nemuselo být možné bez zřejmého vztažného bodu.

Obecné hledání vzájemných posunů objektů lze realizovat pomocí metod detekce a separace struktur a jejich následným porovnáním. Tato metoda nicméně vyžaduje, aby struktury v obraze byly jasně rozpoznatelné a a definované. Na druhou stranu na korelaci založené metody, které jsou dále popisovány v této práci, umějí rozpoznat translaci ztěží viditelných nebo i okem nerozeznatelných objektů (například při vysokém dynamickém rozsahu). Tyto metody však nemají dobré výsledky, nebo je nelze vůbec použít, pro obrazy pořízené s rozdílnou délkou expozice.

Korelační metody používané pro sledování pohybu jediného objektu používají převážně fázovou korelaci. Fázová korelace je křížová korelace po znormování. Toto normování korelační funkce posunutých obrazů přináší zřejmé matematické výsledky v podobě Dirakovy distribuce, což vede k vysoké přesnosti registrace obrazu. Při monitorování pohybu více objektů však toto normování již k tak zřejmým výsledkům nevede, proto se v odvozování matematického aparátu omezujeme výhradně na křížovou korelaci. V implementaci pak ale fázovou korelaci používáme, protože i přes to, že nemá tak zřejmé matematické odůvodnění, jako v případě jediného objektu, pomáhá ke zpřesnění výsledků při hledání posuvů.

Fázová i křížová korelace pracují s Fourierovy spektry obrazů, proto druhou kapitolu dedikujeme popisu Fourierovy transformace a jejích vlastností. Ukazujeme, jakým způsobem působí Fourierova transformace na posunuté obrazy a na obrazy s posunutými objekty. Definujeme zde i konvoluci funkcí a jakým způsobem je křížová korelace konvertibilní na konvoluci. Všechny tyto koncepty představujeme prostředky funkcionální analýzy ve spojitém tvaru.

Nicméně v programové implementaci používáme algoritmus Rychlé Fourierovy transformace (FFT), který využívá diskrétní Fourierovu transformaci. Proto třetí kapitola představuje všechny koncepty uvedené v druhé kapitole v diskrétním případě. Ke korektnímu definování všech těchto pojmů navíc zavádíme periodizaci funkce a představujeme digitální obraz jako diskrétní funkci definovanou na konečném počtu bodů uspořádaných ekvidistantně do čtverce.

Čtvrtá kapitola pak popisuje samotnou počítačovou implementaci odvozených metod. Nejprve popisujeme metody hledání posuvů pro jediný objekt, které jsou detailně popsány ve zdrojích (především [1]). Popisujeme nutnost úpravy vstupních obrazů, a to především jejich tvar a nutnost použití Hanningova okna k ošetření okrajů obrazů. Následně definujeme i váhové funkce, které aplikujeme na Fourierova spektra obrazů k tomu, aby upravily tvar funkce fázové korelace pro vyšší přesnost. Ukazujeme i momentovou metodou hledání posunů pro sub-pixelovou přesnost výsledků. Následně představujeme algoritmus pro hledání posuvů více objektů jako modifikaci algoritmu pro hledání translace jediného objektu. Posuvy hledáme jako lokální maxima funkce fázové korelace a to tak, že hledáme maximum globální, které po zaznamenání výsledku smažeme a hledáme další. Nakonec testujeme přesnost implementovaného algoritmu a ospravedlňujeme tvrzení, že automatizace procesu hledání posuvů více objektů užitím křížové korelace není možná.

I declare that I have written the master's thesis *Following of multiple object movement by means of cross correlation* on my own, according to advice of my master's thesis supervisor prof. RNDr. Miloslav Druckmüller, CSc.,and using the sources listed in references.

April 20,2019 Eliška Málková

I would like to express thanks to my master's thesis supervisor prof. RNDr. Miloslav Druckmüller, CSc. for help with writing of my thesis, for very competent and quick help with all my problems.

Eliška Málková

# Contents

# Chapter 1

# Introduction

The Following of multiple object movement can be used in studies of microscopic particles transport in cells, or to describe the movement and social behaviour of organisms in the group. It can also be used to observe the mutual movement of space objects or to analyse the records taken by traffic surveillance system.

The Following of multiple object movement by means of cross-correlation is generalization of the Finding mutual shift of shifted images (that means the Following of the movement of single object, which is whole image). On the other hand to the standard image registration (e.g. recognizes shifts, rotation and scale), we are working only with translational movement represented by shift vectors. It could not be possible to find rotations and scales of the multiple objects without clear reference point.

The mutual shift search can be executed by the identification of object structures in the image and matching them separately to be followed. However, this method requires the structures to be clearly visible in the image. On the other hand, the correlation based method (described further in this thesis), can even recognize the movement of barely or not visible structures. It is inapplicable to images with different exposition though.

The correlation method of the translational movement analysis generally uses the phase-correlation function. It demonstrates the results with high precision if used to follow the movement of a single object. However, to follow the multiple objects movement we need to use the cross-correlation function, because the norming of spectra does not bring as clear mathematical results as in one object case. Despite this fact, the phase-correlation function is used in the implementation. Reasons to do so are enlisted in Chapter 4.

The phase-correlation uses the Fourier spectra of the images, therefore we are devoting the Chapter 2 to introduction of the Fourier transform and its properties in $\mathbb{R}^2$. However, we use the Fast Fourier transform algorithm, which is the implementation of the discrete Fourier transform, in computer programs implementation of the phase-correlation function. Therefore, we are dedicating Chapter 3 to describe the discrete Fourier transform and its properties for functions defined on a finite number of points (which arranged in square represent the digital image) together with cross-correlation and phase-correlation function. Chapter 4 deals with implementation of the above mentioned method in computer program for one object at first (based on the source [1]), then with implementation of the adjustments of this method to follow the multiple objects movement.

# Chapter 2

# The Fourier transform

At first, we will establish all the theory for the continuous functions. Despite the fact that the digital image is not continuous but discrete, we will summarize the theory for well known continuous functions in the first distance. In that case we can use the conclusions of the Mathematical and Functional analysis.

## 2.1 Basic notions

First of all, let us define some basic concepts, which will be used in the following text. There will be mostly concepts used in Functional analysis and they will not be defined with proper background. Yet the related mathematical theory can be found in sources mentioned in each definition. The exactness of the unmentioned mathematical theory is not essential for purposes of this thesis, it serves mainly for deeper understanding. Therefore, it is omitted.

**Definition 2.1. (Improper double integral)**[1] Let $f(x,y)$ be a function $\mathbb{R}^2 \longrightarrow \mathbb{C}$. Let $R = \langle a, \infty) \times \langle c, \infty), a, c \in \mathbb{R}$. If the following limits exist and are equal

$$\lim_{(b,d)\longrightarrow(\infty,\infty)} \int_a^b \left( \int_c^d f(x,y)\mathrm{d}y \right) \mathrm{d}x = \lim_{(b,d)\longrightarrow(\infty,\infty)} \int_c^d \left( \int_a^b f(x,y)\mathrm{d}x \right) \mathrm{d}y = A,$$

then we define

$$\iint_R f(x,y)\mathrm{d}x\mathrm{d}y = A.$$

Analogically, the integral is defined for $R = (-\infty, b\rangle \times \langle c, \infty)$, $R = \langle a, \infty) \times (-\infty, d\rangle$ and $R = (-\infty, b\rangle \times (-\infty, d\rangle$. Furthermore, if all the following integrals exist and are

finite (or in case some integral are infinite, they have same sign)

$$\begin{aligned}\iint\limits_{\langle 0,\infty)^2} f(x,y)\mathrm{d}x\mathrm{d}y &= B,\\ \iint\limits_{(-\infty,0\rangle\times\langle 0,\infty)} f(x,y)\mathrm{d}x\mathrm{d}y &= C,\\ \iint\limits_{\langle 0,\infty)\times(-\infty,0\rangle} f(x,y)\mathrm{d}x\mathrm{d}y &= D,\\ \iint\limits_{(-\infty,0\rangle^2} f(x,y)\mathrm{d}x\mathrm{d}y &= E,\end{aligned}$$

we define

$$\int\limits_{-\infty}^{\infty}\int\limits_{-\infty}^{\infty} f(x,y)\mathrm{d}x\mathrm{d}y = \iint\limits_{(-\infty,\infty)^2} f(x,y)\mathrm{d}x\mathrm{d}y = B+C+D+E.$$

**Definition 2.2. (Dirac distribution)**[9] The two dimensional *Dirac distribution* is a functional on the basic space. It is singular distribution and is represented by the integral identity with testing function $\varphi(x,y)$ as follows:

$$\int\limits_{-\infty}^{\infty}\int\limits_{-\infty}^{\infty} \delta(x,y)\varphi(x,y)\mathrm{d}x\mathrm{d}y = \varphi(0,0).$$

Where $\delta(x,y)$ fulfils

$$\int\limits_{-\infty}^{\infty}\int\limits_{-\infty}^{\infty} \delta(x,y)\mathrm{d}x\mathrm{d}y = 1,\ \delta(x,y) = 0 \quad \text{if} \quad (x,y)\neq(0,0).$$

More about functionals, basic space and distributions can be found in [9].

## 2.2 The Fourier transform and inverse Fourier transform

The Fourier transform is the essential mathematical instrument in the Image analysis. Because the image is two dimensional, we omit the one dimensional case completely. Therefore, we are using the two dimensional case directly.

**Definition 2.3. (The Fourier transform of functions in $\mathcal{L}(\mathbb{R}^2)$)**[8] Let $f(x,y)\in\mathcal{L}(\mathbb{R}^2)$. The *Fourier transform* of function $f$ is a function $\mathcal{F}\{f\}(\xi,\eta) = F(\xi,\eta):\mathbb{R}^2\longrightarrow\mathbb{C}$ defined as

$$F(\xi,\eta) = \int\limits_{-\infty}^{\infty}\int\limits_{-\infty}^{\infty} f(x,y)\mathrm{e}^{-\mathrm{i}(x\xi+y\eta)}\mathrm{d}x\mathrm{d}y.$$

Function $F$ is also called the *Fourier spectrum* of function $f$.

**Definition 2.4. (Inverse Fourier transform of functions in $\mathcal{L}(\mathbb{R}^2)$)**[8] Let function $G(\xi,\eta) \in \mathcal{L}(\mathbb{R}^2)$. The *inverse Fourier transform* of function $G$ is a function $\mathcal{F}^{-1}\{G\}(x,y) = g(x,y) : \mathbb{R}^2 \longrightarrow \mathbb{C}$ defined as

$$g(x,y) = \frac{1}{4\pi^2} \int_{-\infty}^{\infty}\int_{-\infty}^{\infty} G(\xi,\eta)\mathrm{e}^{\mathrm{i}(x\xi+y\eta)}\mathrm{d}\xi\mathrm{d}\eta.$$

The Fourier transform and also inverse Fourier transform exist and are bounded functions ([1]). However, the inverse Fourier transform of the Fourier spectrum of some function in $\mathcal{L}(\mathbb{R}^2)$ may not even be defined or it could happen that $\mathcal{F}^{-1}\{\mathcal{F}\{f(x,y)\}\} \neq f(x)$. The previous inequality can be shown on functions $f(x,y)$ and $g(x,y)$ which differ on set of cardinality zero. They have the same Fourier transform which obviously leads to mentioned inequality.

**Theorem 2.5. (Fourier inversion theorem for functions in $\mathcal{L}(\mathbb{R}^2)$)** [7] If function $f(\xi,\eta) \in \mathcal{L}(\mathbb{R}^2)$ and is continuous on $\mathbb{R}^2$, then for every $(\xi,\eta) \in \mathbb{R}^2$ holds

$$f(x,y) = \lim_{\epsilon\to 0} \frac{1}{4\pi^2} \int_{-\infty}^{\infty}\int_{-\infty}^{\infty} F(\xi,\eta)\mathrm{e}^{\mathrm{i}(x\xi+y\eta)}\mathrm{e}^{-\epsilon^2\frac{\xi^2+\eta^2}{2}}\mathrm{d}\xi\mathrm{d}\eta.$$

If also $F(\xi,\eta) \in \mathcal{L}(\mathbb{R}^2)$ then

$$\mathcal{F}^{-1}\{\mathcal{F}\{f(x,y)\}\} = \frac{1}{4\pi^2} \int_{-\infty}^{\infty}\int_{-\infty}^{\infty} F(\xi,\eta)\mathrm{e}^{\mathrm{i}(x\xi+y\eta)}\mathrm{d}\xi\mathrm{d}\eta = f(x,y).$$

*Proof.* A proof and its general derivation can be found in [6]. □

## 2.3 Shift theorem

In this section, we are defining the shifted function, the function consisting of objects and the function with shifted objects. They are all defined to best suit the continuous representation of digital image. The shift theorems follow the definitions of shifted function and function with shifted objects to show, how the Fourier transform works applied to these functions. We will consider the function to have just two objects at first and show the general $n$-object case after that.

**Definition 2.6. (Shifted function)** Let $f(x,y) \in \mathcal{L}(\mathbb{R}^2)$ and let $x_0, y_0 \in \mathbb{R}$ given numbers. The function $f_{sh}(x,y)$ is *shifted function* of function $f(x,y)$ by $x_0$ in $x$ axis and by $y_0$ in $y$ axis iff

$$f_{sh}(x,y) = f(x-x_0, y-y_0).$$

The vector $(x_0,y_0)$ is called *shift vector*.

**Theorem 2.7. (Shift theorem)** Let $f(x,y) \in \mathcal{L}(\mathbb{R}^2)$, let $F(\xi,\eta)$ be its Fourier spectrum and let $f_{sh}(x,y)$ be its shifted function by vector $(x_0,y_0)$. Let $F_{sh}(\xi,\eta)$ be the Fourier spectrum of the shifted function $f_{sh}(x,y)$. Then it holds

$$F_{sh}(\xi,\eta) = F(\xi,\eta)\mathrm{e}^{-\mathrm{i}(\xi x_0+\eta y_0)}.$$

*Proof.* The proof taken from [1].

$$\begin{aligned} F_{sh}(\xi,\eta) &= \int_{-\infty}^{\infty}\int_{-\infty}^{\infty} f(x-x_0,y-y_0)\mathrm{e}^{-\mathrm{i}(x\xi+y\eta)}\mathrm{d}x\mathrm{d}y = \\ &= \left|\begin{array}{cccc} s=x-x_0 & x=s+x_0 & \mathrm{d}s=\mathrm{d}x \\ t=y-y_0 & y=t+y_0 & \mathrm{d}t=\mathrm{d}y \end{array}\right| = \\ &= \int_{-\infty}^{\infty}\int_{-\infty}^{\infty} f(s,t)\mathrm{e}^{-\mathrm{i}(\xi(s+x_0)+\eta(t+y_0))}\mathrm{d}s\mathrm{d}t = \\ &= \int_{-\infty}^{\infty}\int_{-\infty}^{\infty} f(s,t)\mathrm{e}^{-\mathrm{i}(s\xi+t\eta)}\mathrm{e}^{-\mathrm{i}(\xi x_0+\eta y_0)}\mathrm{d}s\mathrm{d}t = F(\xi,\eta)\mathrm{e}^{-\mathrm{i}(\xi x_0+\eta y_0)}. \end{aligned}$$

□

**Definition 2.8. (Multiple objects in function)** Let $n \in \mathbb{N}$ be given number, let function $f(x,y) \in \mathcal{L}(\mathbb{R}^2)$ and also functions $f_i(x,y) \in \mathcal{L}(\mathbb{R}^2)$ for each $i = 1,2,\ldots n$. Function $f(x,y)$ consist of $n$ objects iff

$$f(x,y) = \sum_{i=1}^{n} f_i(x,y).$$

We call functions $f_i(x,y)$ the *objects*.

The function with multiple objects is defined as continuous case of multiple objects in the image. The objects in an image are often represented by set of pixels which always move together (they all have the same shift vector), or on the contrary are stationary considering other objects (i.e. background). So the object defined on $\mathbb{R}^2$ is represented by function $f_i(x,y)$ which is non-zero on the object set and zero elsewhere. This guarantees that in the summation, the object's values are not changed (we are only adding zero, because the objects are not overlapping). For purposes of this thesis we will distinguish only objects which have different shift than the rest of the image.

**Definition 2.9. (Function with shifted objects)** Let $f(x,y)$ be a function with $n$ objects, let $x_i, y_i \in \mathbb{R}$ given numbers for each $i = 1,2,\ldots n$. Function $g(x,y)$ is *function with shifted objects* considering $f(x,y)$ iff

$$g(x,y) = \sum_{i=1}^{n} f_i(x-x_i, y-y_i).$$

We say that object $i$ is shifted by vector $(x_i, y_i)$.

Let us remark that each object $f_i(x,y)$ of function $f(x,y)$ is shifted in function $g(x,y)$. Therefore, we can say that objects $f_{i,sh}(x,y) = f_i(x-x_i, y-y_i)$ are shifted functions of functions (objects) $f_i(x,y)$ by vectors $(x_i, y_i)$. Also considering $n = 1$, we are obtaining the definition of the shifted function. So we can say, that the shifted function consists of only one object, which is shifted.

**Theorem 2.10. (Shift theorem for functions with two objects)** Let $f(x,y)$ be a function with two objects ($n = 2$), let $F_1(\xi,\eta)$ and $F_2(\xi,\eta)$ be Fourier spectra of its objects $f_1(x,y), f_2(x,y)$. Let $g(x,y)$ be function with shifted objects considering $f(x,y)$ and let $G(\xi,\eta)$ be its Fourier spectrum. Then it holds

$$G(\xi,\eta) = F_1(\xi,\eta)\mathrm{e}^{-\mathrm{i}(\xi x_1+\eta y_1)} + F_2(\xi,\eta)\mathrm{e}^{-\mathrm{i}(\xi x_2+\eta y_2)}.$$

*Proof.*

$$
\begin{aligned}
G(\xi,\eta) &= \int_{-\infty}^{\infty}\int_{-\infty}^{\infty} g(x,y)\mathrm{e}^{-\mathrm{i}(x\xi+y\eta)}\mathrm{d}x\mathrm{d}y = \\
&= \int_{-\infty}^{\infty}\int_{-\infty}^{\infty} (f_1(x-x_1,y-y_1)+f_2(x-x_2,y-y_2))\mathrm{e}^{-\mathrm{i}(x\xi+y\eta)}\mathrm{d}x\mathrm{d}y = \\
&= \int_{-\infty}^{\infty}\int_{-\infty}^{\infty} f_1(x-x_1,y-y_1)\mathrm{e}^{-\mathrm{i}(x\xi+y\eta)}\mathrm{d}x\mathrm{d}y + \\
&+ \int_{-\infty}^{\infty}\int_{-\infty}^{\infty} f_2(x-x_2,y-y_2)\mathrm{e}^{-\mathrm{i}(x\xi+y\eta)}\mathrm{d}x\mathrm{d}y = \\
&= \left|\begin{array}{lll} s=x-x_1 & x=s+x_1 & \mathrm{d}s=\mathrm{d}x \\ t=y-y_1 & y=t+y_1 & \mathrm{d}t=\mathrm{d}y \\ u=x-x_2 & x=u+x_2 & \mathrm{d}u=\mathrm{d}x \\ v=y-y_2 & y=v+y_2 & \mathrm{d}v=\mathrm{d}y \end{array}\right| = \\
&= \int_{-\infty}^{\infty}\int_{-\infty}^{\infty} f_1(s,t)\mathrm{e}^{-\mathrm{i}((s+x_1)\xi+(t+y_1)\eta)}\mathrm{d}s\mathrm{d}t + \\
&+ \int_{-\infty}^{\infty}\int_{-\infty}^{\infty} f_2(u,v)\mathrm{e}^{-\mathrm{i}((u+x_2)\xi+(v+y_2)\eta)}\mathrm{d}u\mathrm{d}v = \\
&= \int_{-\infty}^{\infty}\int_{-\infty}^{\infty} f_1(s,t)\mathrm{e}^{-\mathrm{i}(s\xi+t\eta)}\mathrm{e}^{-\mathrm{i}(x_1\xi+y_1\eta)}\mathrm{d}s\mathrm{d}t + \\
&+ \int_{-\infty}^{\infty}\int_{-\infty}^{\infty} f_2(u,v)\mathrm{e}^{-\mathrm{i}(u\xi+v\eta)}\mathrm{e}^{-\mathrm{i}(x_2\xi+y_2\eta)}\mathrm{d}u\mathrm{d}v = \\
&= F_1(\xi,\eta)\mathrm{e}^{-\mathrm{i}(\xi x_1+\eta y_1)} + F_2(\xi,\eta)\mathrm{e}^{-\mathrm{i}(\xi x_2+\eta y_2)}.
\end{aligned}
$$

□

**Theorem 2.11. (Shift theorem for functions with $n$ objects)** Let $f(x,y)$ be a function with $n$ objects and let $F_i(\xi,\eta)$ be Fourier spectra of objects $f_i(x,y)$ for each $i = 1,2,\dots n$. Let $g(x,y)$ be function with shifted objects considering $f(x,y)$ and let $G(\xi,\eta)$ be its Fourier spectrum. Then it holds

$$G(\xi,\eta) = \sum_{i=1}^{n} F_i(\xi,\eta)\mathrm{e}^{-\mathrm{i}(x_i\xi+y_i\eta)}.$$

*Proof.* Proof can be derived as outward generalization of proof of the Theorem 2.10. □

## 2.4 Properties of Fourier transform

Let us introduce some basic properties of the Fourier transform. They are not essential for finding the shifts of the images, but they are used in some of the proves that follow in next sections.

**Theorem 2.12.** Let $f(x,y) \in \mathcal{L}(\mathbb{R}^2)$ and let $F(\xi,\eta)$ be its Fourier spectrum. Then

$$\mathcal{F}\{f(-x,-y)\} = F(-\xi,-\eta).$$

*Proof.*

$$\begin{aligned} F(-\xi,-\eta) &= \left| \begin{array}{l} \sigma = -\xi \\ \tau = -\eta \end{array} \right| = F(\sigma,\tau) = \int_{-\infty}^{\infty}\int_{-\infty}^{\infty} f(s,t)\mathrm{e}^{-\mathrm{i}(s\sigma+t\tau)}\mathrm{d}s\mathrm{d}t = \\ &= \int_{-\infty}^{\infty}\int_{-\infty}^{\infty} f(s,t)\mathrm{e}^{-\mathrm{i}(-s\xi-t\eta)}\mathrm{d}s\mathrm{d}t = \left| \begin{array}{ll} x = -s & \mathrm{d}x = -\mathrm{d}s \\ t = -y & \mathrm{d}t = -\mathrm{d}y \end{array} \right| = \\ &= \int_{-\infty}^{\infty}\int_{-\infty}^{\infty} f(-x,-y)\mathrm{e}^{-\mathrm{i}(x\xi+y\eta)}\mathrm{d}x\mathrm{d}y = \mathcal{F}\{f(-x,-y)\}. \end{aligned}$$

□

This theorem is just special case of Scale-change theorem if we consider $\alpha = -1$. It says that $\mathcal{F}\{f(\alpha x,\alpha y)\} = \frac{1}{\alpha^2}F\left(\frac{\xi}{\alpha},\frac{\eta}{\alpha}\right)$. The exact formulation of Scale-change theorem can be found together with its proof in [1].

**Theorem 2.13.** [5] Let function $f \in \mathcal{L}(\mathbb{R}^2)$. Then

(a) $\mathcal{F}\{f(x,y)\} = 4\pi^2\mathcal{F}^{-1}\{f(-x,-y)\}$,

(b) $\mathcal{F}^{-1}\{f(x,y)\} = \frac{1}{4\pi^2}\mathcal{F}\{f(-x,-y)\}$.

If $f$ is also continuous and its Fourier spectrum $F(\xi,\eta) \in \mathcal{L}(\mathbb{R}^2)$, then

(c) $\mathcal{F}\{\mathcal{F}\{f(x,y)\}\} = 4\pi^2 f(-x,-y)$,

(d) $\mathcal{F}^{-1}\{\mathcal{F}^{-1}\{f(x,y)\}\} = \frac{1}{4\pi^2}f(-x,-y)$.

*Proof.* Proof taken from [1].

(a)

$$\begin{aligned} 4\pi^2\mathcal{F}^{-1}\{f(-x,-y)\} &= 4\pi^2\frac{1}{4\pi^2}\int_{-\infty}^{\infty}\int_{-\infty}^{\infty} f(-x,-y)\mathrm{e}^{\mathrm{i}(x\xi+y\eta)}\mathrm{d}x\mathrm{d}y = \\ &= \left| \begin{array}{ll} s = -x & \mathrm{d}s = -\mathrm{d}x \\ t = -y & \mathrm{d}t = -\mathrm{d}y \end{array} \right| = \\ &= \int_{-\infty}^{\infty}\int_{-\infty}^{\infty} f(s,t)\mathrm{e}^{-\mathrm{i}(s\xi+t\eta)}\mathrm{d}s\mathrm{d}t = \mathcal{F}\{f(x,y)\}. \end{aligned}$$

(b)

$$\begin{aligned}
&\mathcal{F}\{f(x,y)\} = 4\pi^2\mathcal{F}^{-1}\{f(-x,-y)\} \qquad \Big\backslash \cdot\frac{1}{4\pi^2}\\
&\frac{1}{4\pi^2}\mathcal{F}\{f(x,y)\} = \mathcal{F}^{-1}\{f(-x,-y)\}\\
&\frac{1}{4\pi^2}\mathcal{F}\{f(-x,-y)\} = \mathcal{F}^{-1}\{f(x,y)\}
\end{aligned}$$

The last equality was obtained by substituting $-x$ for $x$ and $-y$ for $y$.

(c)

$$\begin{aligned}
\mathcal{F}\{\mathcal{F}\{f(x,y)\}\} &= \int_{-\infty}^{\infty}\int_{-\infty}^{\infty} F(\xi,\eta)\mathrm{e}^{-\mathrm{i}(x\xi+y\eta)}\mathrm{d}\xi\mathrm{d}\eta =\\
&= \int_{-\infty}^{\infty}\int_{-\infty}^{\infty} F(\xi,\eta)\mathrm{e}^{\mathrm{i}(x(-\xi)+y(-\eta)}\mathrm{d}\xi\mathrm{d}\eta =\\
&= \left|\begin{array}{ll}\sigma=-\xi & \mathrm{d}\sigma=-\mathrm{d}\xi\\ \tau=-\eta & \mathrm{d}\tau=-\mathrm{d}\eta\end{array}\right| = \int_{-\infty}^{\infty}\int_{-\infty}^{\infty} F(-\sigma,-\tau)\mathrm{e}^{\mathrm{i}(x\sigma+y\tau)}\mathrm{d}\sigma\mathrm{d}\tau =\\
&= 4\pi^2\mathcal{F}^{-1}\{\mathcal{F}\{f(-x,-y)\}\} = 4\pi^2 f(-x,-y).
\end{aligned}$$

(d)

$$\mathcal{F}^{-1}\{\mathcal{F}^{-1}\{f(x,y)\}\} = \frac{1}{4\pi^2}\int_{-\infty}^{\infty}\int_{-\infty}^{\infty}\left(\frac{1}{4\pi^2}\int_{-\infty}^{\infty}\int_{-\infty}^{\infty} f(s,t)\mathrm{e}^{\mathrm{i}(s\xi+t\eta)}\mathrm{d}s\mathrm{d}t\right)\mathrm{e}^{\mathrm{i}(x\xi+y\eta)}\mathrm{d}\xi\mathrm{d}\eta =$$

$$\begin{aligned}
&= \frac{1}{16\pi^4}\int_{-\infty}^{\infty}\int_{-\infty}^{\infty}\left(\int_{-\infty}^{\infty}\int_{-\infty}^{\infty} f(s,t)\mathrm{e}^{-\mathrm{i}(-s\xi-t\eta)}\mathrm{d}s\mathrm{d}t\right)\mathrm{e}^{i(x\xi+y\eta)}\mathrm{d}\xi\mathrm{d}\eta =\\
&= \left|\begin{array}{ll}u=-s & \mathrm{d}u=-\mathrm{d}s\\ v=-t & \mathrm{d}v=-\mathrm{d}t\end{array}\right| =\\
&= \frac{1}{16\pi^4}\int_{-\infty}^{\infty}\int_{-\infty}^{\infty}\left(\int_{-\infty}^{\infty}\int_{-\infty}^{\infty} f(-u,-v)\mathrm{e}^{-\mathrm{i}(u\xi+v\eta)}\mathrm{d}u\mathrm{d}v\right)\mathrm{e}^{i(x\xi+y\eta)}\mathrm{d}\xi\mathrm{d}\eta =\\
&= \frac{1}{4\pi^2}\mathcal{F}^{-1}\{\mathcal{F}\{f(-x,-y)\}\} = \frac{1}{4\pi^2}f(-x,-y).
\end{aligned}$$

□

**Example 2.14.** [5] Let us consider $f(x,y) = \delta(x-x_0, y-y_0)$. Then the Fourier transform of the shifted Dirac distribution can be computed as

$$\mathcal{F}\{\delta(x-x_0,y-y_0)\} = \int_{-\infty}^{\infty}\int_{-\infty}^{\infty}\delta(x-x_0,y-y_0)\mathrm{e}^{-\mathrm{i}(x\xi+y\eta)}\mathrm{d}x\mathrm{d}y = \mathrm{e}^{-\mathrm{i}(x_0\xi+y_0\eta)}.$$

Next let us consider $f(x,y) = \mathrm{e}^{\mathrm{i}(x_0x+y_0y)}$. Then the Fourier transform of this function can by computed as

$$\begin{aligned}\mathcal{F}\{\mathrm{e}^{\mathrm{i}(x_0x+y_0y)}\} &= \int_{-\infty}^{\infty}\int_{-\infty}^{\infty} \mathrm{e}^{\mathrm{i}(x_0x+y_0y)}\mathrm{e}^{-\mathrm{i}(x\xi+y\eta)}\mathrm{d}x\mathrm{d}y = \\ &= \int_{-\infty}^{\infty}\int_{-\infty}^{\infty} \mathrm{e}^{-\mathrm{i}(x(\xi-x_0)+y(\eta-y_0))}\mathrm{d}x\mathrm{d}y = \delta(\xi-x_0,\eta-y_0).\end{aligned}$$

This is more generally shown in [5].

**Theorem 2.15.** [5] Let $f(x,y) \in \mathcal{L}(\mathbb{R}^2)$ and $F(\xi,\eta)$ be its Fourier spectrum. The Fourier spectrum of the complex conjugate of function $f$ is the complex conjugate of its Fourier spectra with reversed axes

$$\mathcal{F}\{f^*(x,y)\} = F^*(-\xi,-\eta).$$

*Proof.* Proof taken from [5].

$$\begin{aligned}\mathcal{F}\{f^*(x,y)\} &= \int_{-\infty}^{\infty}\int_{-\infty}^{\infty} f^*(x,y)\mathrm{e}^{-\mathrm{i}(x\xi+y\eta)}\mathrm{d}x\mathrm{d}y = \int_{-\infty}^{\infty}\int_{-\infty}^{\infty} f^*(x,y)\mathrm{e}^{\mathrm{i}(-x\xi-y\eta)}\mathrm{d}x\mathrm{d}y = \\ &= \left(\int_{-\infty}^{\infty}\int_{-\infty}^{\infty} f(x,y)\mathrm{e}^{-\mathrm{i}(x(-\xi)+y(-\eta))}\mathrm{d}x\mathrm{d}y\right)^* = F^*(-\xi,-\eta),\end{aligned}$$

where the third equality holds because for $a \in \mathbb{R}$ is $\mathrm{e}^{\mathrm{i}a} = \cos a + \mathrm{i}\sin a$, $\mathrm{e}^{-\mathrm{i}a} = \cos a + \mathrm{i}\sin(-a) = \cos a - \mathrm{i}\sin a$. Hence $\mathrm{e}^{\mathrm{i}a} = \left(\mathrm{e}^{-\mathrm{i}a}\right)^*$. □

**Theorem 2.16.** [5] Let $f(x,y) \in \mathcal{L}(\mathbb{R}^2)$ and continuous, let $F(\xi,\eta) \in \mathcal{L}(\mathbb{R}^2)$ its Fourier spectrum. Then the inverse Fourier transform of the complex conjugate of spectrum $F$ is the complex conjugate of function $f$ with reversed axes, i.e. in every point where $f$ is continuous it holds

$$\mathcal{F}^{-1}\{F^*(\xi,\eta)\} = f^*(-x,-y).$$

*Proof.* Proof taken from [5].

$$\begin{aligned}\mathcal{F}^{-1}\{F^*(\xi,\eta)\} &= \frac{1}{4\pi^2}\int_{-\infty}^{\infty}\int_{-\infty}^{\infty} F^*(\xi,\eta)\mathrm{e}^{\mathrm{i}(x\xi+y\eta)}\mathrm{d}\xi\mathrm{d}\eta = \\ &= \frac{1}{4\pi^2}\int_{-\infty}^{\infty}\int_{-\infty}^{\infty} F^*(\xi,\eta)\mathrm{e}^{-\mathrm{i}(-x\xi-y\eta)}\mathrm{d}\xi\mathrm{d}\eta = \\ &= \left(\frac{1}{4\pi^2}\int_{-\infty}^{\infty}\int_{-\infty}^{\infty} F(\xi,\eta)\mathrm{e}^{\mathrm{i}(x(-\xi)+y(-\eta))}\mathrm{d}\xi\mathrm{d}\eta\right)^* = f^*(-x,-y).\end{aligned}$$

□

**Theorem 2.17.** [1] Let $f(x,y) \in \mathcal{L}(\mathbb{R}^2)$ and continuous, let $F(\xi,\eta) \in \mathcal{L}(\mathbb{R}^2)$ its Fourier spectrum. Function $f$ is real function (i.e. $f(x,y) = f^*(x,y) \quad \forall (x,y) \in \mathbb{R}^2$) iff $F(\xi,\eta) = F^*(-\xi,-\eta)$.

*Proof.* Proof taken from [5]

1. Let us suppose that $f$ is real function. Then it holds

$$F(\xi,\eta) = \mathcal{F}\{f(x,y)\} = \mathcal{F}\{f^*(x,y)\} = F^*(-\xi,-\eta).$$

2. Let us suppose that $F(\xi,\eta) = F^*(-\xi,-\eta)$.Then it holds

$$f(x,y) = \mathcal{F}^{-1}\{F(\xi,\eta)\} = \mathcal{F}^{-1}\{F^*(-\xi,-\eta)\} = f^*(x,y).$$

□

**Corollary 2.18.** [1] Let $f(x,y) \in \mathcal{L}(\mathbb{R}^2)$ be a real continuous function with a Fourier spectrum $F(\xi,\eta) \in \mathcal{L}(\mathbb{R}^2)$. Let $G(\xi,\eta)$ be a bounded function $\mathbb{R}^2 \longrightarrow \mathbb{R}$ such that $G(\xi,\eta) = G(-\xi,-\eta)$. Then

$$\mathcal{F}^{-1}\{F(\xi,\eta)\cdot G(\xi,\eta)\}$$

is real.

*Proof.* Proof taken from [1]. If $f$ is real, then according to Theorem 2.17 it holds

$$F(\xi,\eta) = F^*(-\xi,-\eta).$$

Multiplying the equality by $G$ we obtain

$$F(\xi,\eta)\cdot G(\xi,\eta) = F^*(-\xi,-\eta)\cdot G(-\xi,-\eta) = (F(-\xi,-\eta)\cdot G(-\xi,-\eta))^*.$$

Since $G$ is bounded, there is no doubt about existence of the inverse Fourier transform. And according to the Theorem 2.17 again,

$$\mathcal{F}\{F(\xi,\eta)\cdot G(\xi,\eta)\}$$

is real. □

## 2.5 Convolution and its properties

The convolution is often used in the Image analysis because of its compatibility with the Fourier transform which is shown int Theorems 2.22. and 2.23..

**Definition 2.19. (Convolution)**[8] Let functions $f(x,y), g(x,y) \in \mathcal{L}(\mathbb{R}^2)$. The *convolution* of functions $f, g$ is function

$$h(x,y) = f(x,y) * g(x,y) = \int_{-\infty}^{\infty}\int_{-\infty}^{\infty} f(s,t)g(x-s,y-t)\mathrm{d}s\mathrm{d}t.$$

**Theorem 2.20.** [1] Let functions $f(x,y), g(x,y) \in \mathcal{L}(\mathbb{R}^2)$. Then $f * g \in \mathcal{L}(\mathbb{R}^2)$.

*Proof.* Proof taken from [1]. We start by proving that $f(x,y)\cdot g(u,v) \in \mathcal{L}(\mathbb{R}^4)$, i.e.

$$\int_{-\infty}^{\infty}\int_{-\infty}^{\infty}\int_{-\infty}^{\infty}\int_{-\infty}^{\infty} |f(x,y)g(u,v)|\mathrm{d}u\,\mathrm{d}v\,\mathrm{d}x\,\mathrm{d}y < \infty.$$

Let us tart by

$$\int_{-\infty}^{\infty}\int_{-\infty}^{\infty}\int_{-\infty}^{\infty}\int_{-\infty}^{\infty}|f(x,y)g(u,v)|\mathrm{d}u\,\mathrm{d}v\,\mathrm{d}x\,\mathrm{d}y =$$
$$= \int_{-\infty}^{\infty}\int_{-\infty}^{\infty}\int_{-\infty}^{\infty}\int_{-\infty}^{\infty}|f(x,y)|\cdot|g(u,v)|\mathrm{d}u\,\mathrm{d}v\,\mathrm{d}x\,\mathrm{d}y =$$
$$= \int_{-\infty}^{\infty}\int_{-\infty}^{\infty}|f(x,y)|\left(\int_{-\infty}^{\infty}\int_{-\infty}^{\infty}|g(u,v)|\mathrm{d}u\,\mathrm{d}v\right)\mathrm{d}x\,\mathrm{d}y.$$

Let us denote

$$I = \int_{-\infty}^{\infty}\int_{-\infty}^{\infty}|g(u,v)|\mathrm{d}u\,\mathrm{d}v.$$

Since $g \in \mathcal{L}(\mathbb{R}^2)$ therefore $0 \leq I < \infty$. Hence we can use Fubini's Theorem it holds

$$\int_{-\infty}^{\infty}\int_{-\infty}^{\infty}|f(x,y)|\left(\int_{-\infty}^{\infty}\int_{-\infty}^{\infty}|g(u,v)|\mathrm{d}u\,\mathrm{d}v\right)\mathrm{d}x\,\mathrm{d}y =$$
$$\int_{-\infty}^{\infty}\int_{-\infty}^{\infty}|f(x,y)|\,\mathrm{d}x\,\mathrm{d}y\int_{-\infty}^{\infty}\int_{-\infty}^{\infty}|g(u,v)|\,\mathrm{d}u\,\mathrm{d}v < \infty.$$

Thus $f(x,y)\cdot g(u,v) \in \mathcal{L}(\mathbb{R}^4)$. By making the substitution $u = p - s, x = s, v = q - t$, $y = z$ we obtain

$$\int_{-\infty}^{\infty}\int_{-\infty}^{\infty}\int_{-\infty}^{\infty}\int_{-\infty}^{\infty}f(x,y)g(u,v)\mathrm{d}u\,\mathrm{d}v\,\mathrm{d}x\,\mathrm{d}y = \int_{-\infty}^{\infty}\int_{-\infty}^{\infty}\int_{-\infty}^{\infty}\int_{-\infty}^{\infty}f(s,t)g(p-s,q-t)\mathrm{d}s\,\mathrm{d}t\,\mathrm{d}p\,\mathrm{d}q,$$

which says that function

$$(f*g)(p,q) = \int_{-\infty}^{\infty}\int_{-\infty}^{\infty}f(p-s,q-t)g(s,t)\mathrm{d}s\mathrm{d}t$$

belongs to $\mathcal{L}(\mathbb{R}^2)$. □

**Theorem 2.21.** [1] Let functions $f(x,y), g(x,y) \in \mathcal{L}(\mathbb{R}^2)$ with Fourier spectra $F(\xi,\eta)$, $G(\xi,\eta)$. Then

$$\mathcal{F}\{f(x,y)*g(x,y)\} = F(\xi,\eta)\cdot G(\xi,\eta).$$

*Proof.* Proof taken from [8].

$$\begin{aligned}
\mathcal{F}\{f*g\} &= \int_{-\infty}^{\infty}\int_{-\infty}^{\infty}\left(\int_{-\infty}^{\infty}\int_{-\infty}^{\infty} f(s,t)g(x-s,y-t)\mathrm{d}s\mathrm{d}t\right)\mathrm{e}^{-\mathrm{i}(x\xi+y\eta)}\mathrm{d}x\mathrm{d}y = \\
&= \int_{-\infty}^{\infty}\int_{-\infty}^{\infty}\left(\int_{-\infty}^{\infty}\int_{-\infty}^{\infty} f(s,t)g(x-s,y-t)\mathrm{e}^{-\mathrm{i}(x\xi+y\eta)}\mathrm{d}x\mathrm{d}y\right)\mathrm{d}s\mathrm{d}t = \\
&= \int_{-\infty}^{\infty}\int_{-\infty}^{\infty} f(s,t)\left(\int_{-\infty}^{\infty}\int_{-\infty}^{\infty} g(x-s,y-t)\mathrm{e}^{-\mathrm{i}(x\xi+y\eta)}\mathrm{d}x\mathrm{d}y\right)\mathrm{d}s\mathrm{d}t = \\
&= \left|\begin{array}{lll} p=x-s & x=s+p & \mathrm{d}x=\mathrm{d}p \\ q=y-t & y=t+q & \mathrm{d}y=\mathrm{d}q \end{array}\right| = \\
&= \int_{-\infty}^{\infty}\int_{-\infty}^{\infty} f(s,t)\left(\int_{-\infty}^{\infty}\int_{-\infty}^{\infty} g(p,q)\mathrm{e}^{-\mathrm{i}((p+s)\xi+(q+t)\eta)}\mathrm{d}p\mathrm{d}q\right)\mathrm{d}s\mathrm{d}t = \\
&= \int_{-\infty}^{\infty}\int_{-\infty}^{\infty} f(s,t)\left(\int_{-\infty}^{\infty}\int_{-\infty}^{\infty} g(p,q)\mathrm{e}^{-\mathrm{i}(p\xi+q\eta)}\mathrm{e}^{-\mathrm{i}(s\xi+t\eta)}\mathrm{d}p\mathrm{d}q\right)\mathrm{d}s\mathrm{d}t = \\
&= \int_{-\infty}^{\infty}\int_{-\infty}^{\infty} f(s,t)\mathrm{e}^{-\mathrm{i}(s\xi+t\eta)}\mathrm{d}s\mathrm{d}t\int_{-\infty}^{\infty}\int_{-\infty}^{\infty} g(p,q)\mathrm{e}^{-\mathrm{i}(p\xi+q\eta)}\mathrm{d}p\mathrm{d}q = \\
&= F(\xi,\eta)\cdot G(\xi,\eta).
\end{aligned}$$

□

**Theorem 2.22.** [1] Let functions $f(x,y), g(x,y) \in \mathcal{L}(\mathbb{R}^2)$ and continuous with Fourier spectra $F(\xi,\eta), G(\xi,\eta) \in \mathcal{L}(\mathbb{R}^2)$. Then

$$\mathcal{F}\{f(x,y)\cdot g(x,y)\} = \frac{1}{4\pi^2}F(\xi,\eta) * G(\xi,\eta).$$

*Proof.* Proof taken from [1].

$$\begin{aligned}
\mathcal{F}\{f\cdot g\} &= \int_{-\infty}^{\infty}\int_{-\infty}^{\infty} f(x,y)g(x,y)\mathrm{e}^{-\mathrm{i}(x\xi+y\eta)}\mathrm{d}x\mathrm{d}y = \\
&= \int_{-\infty}^{\infty}\int_{-\infty}^{\infty}\left(\frac{1}{4\pi^2}\int_{-\infty}^{\infty}\int_{-\infty}^{\infty} F(\sigma,\tau)\mathrm{e}^{\mathrm{i}(x\sigma+y\tau)}\mathrm{d}\sigma\mathrm{d}\tau\right) g(x,y)\mathrm{e}^{-\mathrm{i}(x\xi+y\eta)}\mathrm{d}x\mathrm{d}y = \\
&= \frac{1}{4\pi^2}\int_{-\infty}^{\infty}\int_{-\infty}^{\infty} F(\sigma,\tau)\left(\int_{-\infty}^{\infty}\int_{-\infty}^{\infty} g(x,y)\mathrm{e}^{-\mathrm{i}(x(\xi-\sigma)+y(\eta-\tau))}\mathrm{d}x\mathrm{d}y\right)\mathrm{d}\sigma\mathrm{d}\tau = \\
&= \frac{1}{4\pi^2}\int_{-\infty}^{\infty}\int_{-\infty}^{\infty} F(\sigma,\tau)G(\xi-\sigma,\eta-\tau)\mathrm{d}\sigma\mathrm{d}\tau = \frac{1}{4\pi^2}F(\xi,\eta) * G(\xi,\eta).
\end{aligned}$$

□

**Theorem 2.23. (Distributivity of convolution)** Let $f(x,y), g(x,y), h(x,y) \in \mathcal{L}(\mathbb{R}^2)$. Then it holds

$$f(x,y) * (g(x,y) + h(x,y)) = f(x,y) * g(x,y) + f(x,y) * h(x,y).$$

*Proof.* Let us denote $k(x,y) = g(x,y) + h(x,y)$. Then it holds

$$\begin{aligned} f(x,y) * (g(x,y) + h(x,y)) &= f(x,y) * k(x,y) = \int_{-\infty}^{\infty}\int_{-\infty}^{\infty} f(s,t)k(x-s,y-t)\mathrm{d}s\mathrm{d}t = \\ &= \int_{-\infty}^{\infty}\int_{-\infty}^{\infty} f(s,t)(g(x-s,y-t)+h(x-s,y-t))\mathrm{d}s\mathrm{d}t = \\ &= \int_{-\infty}^{\infty}\int_{-\infty}^{\infty} f(s,t)g(x-s,y-t)\mathrm{d}s\mathrm{d}t + \\ &+ \int_{-\infty}^{\infty}\int_{-\infty}^{\infty} f(s,t)h(x-s,y-t)\mathrm{d}s\mathrm{d}t = \\ &= f(x,y) * g(x,y) + f(x,y) * h(x,y). \end{aligned}$$

□

## 2.6 Cross correlation, phase correlation

The phase correlation is the most effective tool for obtaining the shift of two functions. It is normalized cross correlation and the norming is possible only for one object. The norming is based on the suppression of the high frequencies of the Fourier spectrum. However, it is only possible to use the cross correlation for more objects in the function.

**Definition 2.24. (Cross-power spectrum, normalized cross-power spectrum)**[1] Let functions $f(x,y), g(x,y) \in \mathcal{L}(\mathbb{R}^2)$ have Fourier spectra $F(\xi,\eta), G(\xi,\eta)$. The *cross-power spectrum* of functions $f, g$ is function $C_{f,g}(\xi,\eta) : \mathbb{R}^2 \longrightarrow \mathbb{C}$ defined as

$$C_{f,g}(\xi,\eta) = F(\xi,\eta) \cdot G^*(\xi,\eta).$$

The *normalized cross-power spectrum* is function $Z_{f,g}(\xi,\eta) : \mathbb{R}^2 \longrightarrow \mathbb{C}$ defined as

$$Z_{f,g}(\xi,\eta) = \frac{F(\xi,\eta) \cdot G^*(\xi,\eta)}{|F(\xi,\eta) \cdot G(\xi,\eta)|}.$$

**Definition 2.25. (Cross-corelation function, phase-correlation function)**[1] Let functions $f(x,y), g(x,y) \in \mathcal{L}(\mathbb{R}^2)$ have Fourier spectra $F(\xi,\eta), G(\xi,\eta)$. The function $Q_{f,g}(x,y) : \mathbb{R}^2 \longrightarrow \mathbb{C}$ defined as

$$Q_{f,g}(x,y) = \mathcal{F}^{-1}\{C_{f,g}(\xi,\eta)\} = \mathcal{F}^{-1}\{F(\xi,\eta) \cdot G^*(\xi,\eta)\}$$

is called the *cross-correlation function* of functions $f, g$. Function $P_{f,g}(x,y) : \mathbb{R}^2 \longrightarrow \mathbb{C}$ defined as

$$P_{f,g}(x,y) = \mathcal{F}^{-1}\{Z_{f,g}(\xi,\eta)\} = \mathcal{F}^{-1}\left\{\frac{F(\xi,\eta) \cdot G^*(\xi,\eta)}{|F(\xi,\eta) \cdot G(\xi,\eta)|}\right\}$$

is called *phase-correlation function* of functions $f, g$.

**Theorem 2.26. (Cross-correlation function of real functions)**[1] Let functions $f(x,y)$, $g(x,y) \in \mathcal{L}(\mathbb{R}^2)$ continuous real ($f = f^*, g = g^*$) and with Fourier spectra $F(\xi,\eta)$, $G(\xi,\eta) \in \mathcal{L}(\mathbb{R}^2)$. Then the cross-correlation function of these functions is real.

*Proof.* Proof taken from [1]. Using Theorems 2.5, 2.16, 2.22 we can compute

$$\begin{aligned} Q_{f,g}(x,y) &= \mathcal{F}^{-1}\{F(\xi,\eta)\cdot G^*(\xi,\eta)\} = \mathcal{F}^{-1}\{\mathcal{F}\{f(x,y)\}\cdot\mathcal{F}\{g^*(-x,-y)\}\} = \\ &= f(x,y) * g^*(-x,-y) = f(x,y) * g(-x,-y), \end{aligned}$$

which is a real function. □

**Remark 2.27.** Noticeably, the cross-correlation function can by transformed to convolution as follows:

$$Q_{f,g}(x,y) = f(x,y) * g^*(-x,-y) = f(x,y) * g(-x,-y),$$

where $f(x,y), g(x,y) \in \mathcal{L}(\mathbb{R}^2)$ continuous real. This matter of fact is often used for easier computation in the Image analysis. It will also be used as useful property of cross-correlation function in some of following proves.

**Theorem 2.28. (Phase correlation function of shifted functions)**[1] Let $f(x,y) \in \mathcal{L}(\mathbb{R}^2)$ and let $F(\xi,\eta)$ be its Fourier spectrum. Let us consider $f_{sh}(x,y)$ shifted function (see Definition 2.6) of function $f(x,y)$ by vector $(x_0,y_0)$ and let $F_{sh}(\xi,\eta)$ be Fourier spectrum of the shifted function. Then the phase-correlation function of functions $f, f_{sh}$ is Dirac distribution shifted by $(-x_0,-y_0)$

$$P_{f,f_{sh}}(x,y) = \delta(x+x_0, y+y_0).$$

*Proof.* The proof taken from [1]. The Shift Theorem 2.7 implies that

$$Z_{f,f_{sh}}(\xi,\eta) = \frac{F(\xi,\eta)\cdot F^*(\xi,\eta)(\mathrm{e}^{-\mathrm{i}(x_0\xi+y_0\eta)})^*}{|F(\xi,\eta)\cdot F(\xi,\eta)\mathrm{e}^{-\mathrm{i}(x_0\xi+y_0\eta)}|} = \mathrm{e}^{\mathrm{i}(x_0\xi+y_0\eta)}.$$

Therefore

$$\begin{aligned} P_{f,f_{sh}}(x,y) &= \mathcal{F}^{-1}\{Z_{f,f_{sh}}(\xi,\eta)\} = \mathcal{F}^{-1}\{\mathrm{e}^{\mathrm{i}(x_0\xi+y_0\eta)}\} = \\ &= \mathcal{F}^{-1}\{\mathrm{e}^{-\mathrm{i}(\xi(-x_0)+\eta(-y_0))}\} = \delta(x+x_0, y+y_0). \end{aligned}$$

□

Obviously the phase-correlation is the perfect tool for finding mutual shifts of shifted functions. The only remaining task is to find the only non-zero element's coordinates and the shift can be obtained after multiplication with $-1$.

**Theorem 2.29. (Cross-correlation function of shifted functions)** Let $f(x,y) \in \mathcal{L}(\mathbb{R}^2)$ continuous real and let us suppose function $f_{sh}(x,y)$ be shifted function of function $f(x,y)$. Then the cross-correlation function of functions $f, f_{sh}$ has its global maximum in $[-x_0,-y_0]$, i.e.

$$Q_{f,f_{sh}}(x,y) \le Q_{f,f_{sh}}(-x_0,-y_0) \quad \forall (x,y) \in \mathbb{R}^2.$$

*Proof.* The one dimensional proof can be found in [10]. Let us begin with equality

$$\begin{aligned} & (f(s,t) - f(s-x-x_0, t-y-y_0))^2 = \\ = \; & f^2(s,t) - 2f(s,t)f(s-x-x_0, t-y-y_0) + f^2(s-x-x_0, t-y-y_0). \end{aligned}$$

By integrating both sides we obtain

$$\begin{aligned} & \int_{-\infty}^{\infty}\int_{-\infty}^{\infty} (f(s,t) - f(s-x-x_0, t-y-y_0))^2 \,\mathrm{d}s\mathrm{d}t = \\ = \; & \int_{-\infty}^{\infty}\int_{-\infty}^{\infty} f^2(s,t)\mathrm{d}s\mathrm{d}t - 2\int_{-\infty}^{\infty}\int_{-\infty}^{\infty} f(s,t)f(s-x-x_0, t-y-y_0)\mathrm{d}s\mathrm{d}t + \\ + \; & \int_{-\infty}^{\infty}\int_{-\infty}^{\infty} f^2(s-x-x_0, t-y-y_0)\mathrm{d}s\mathrm{d}t. \end{aligned}$$

The last integral can be modified as follows

$$\begin{aligned} \int_{-\infty}^{\infty}\int_{-\infty}^{\infty} f^2(s-x-x_0, t-y-y_0)\mathrm{d}s\mathrm{d}t &= \left| \begin{array}{ll} u = s-x-x_0 & \mathrm{d}u = \mathrm{d}s \\ v = t-y-y_0 & \mathrm{d}v = \mathrm{d}t \end{array} \right| = \\ &= \int_{-\infty}^{\infty}\int_{-\infty}^{\infty} f^2(u,v)\mathrm{d}u\mathrm{d}v = \left| \begin{array}{ll} s = u & \mathrm{d}s = \mathrm{d}u \\ t = v & \mathrm{d}t = \mathrm{d}v \end{array} \right| = \\ &= \int_{-\infty}^{\infty}\int_{-\infty}^{\infty} f^2(s,t)\mathrm{d}s\mathrm{d}t. \end{aligned}$$

Using the modification we obtain

$$\begin{aligned} & \int_{-\infty}^{\infty}\int_{-\infty}^{\infty} f(s,t)f(s-x-x_0, t-y-y_0)\mathrm{d}s\mathrm{d}t = \\ = \; & \int_{-\infty}^{\infty}\int_{-\infty}^{\infty} f^2(s,t)\mathrm{d}s\mathrm{d}t - \frac{1}{2}\int_{-\infty}^{\infty}\int_{-\infty}^{\infty} (f(s,t) - f(s-x-x_0, t-y-y_0))^2 \,\mathrm{d}s\mathrm{d}t. \end{aligned}$$

Since the last integral is non-negative, we can write

$$\int_{-\infty}^{\infty}\int_{-\infty}^{\infty} f(s,t)f(s-x-x_0, t-y-y_0)\mathrm{d}s\mathrm{d}t \leq \int_{-\infty}^{\infty}\int_{-\infty}^{\infty} f^2(s,t)\mathrm{d}s\mathrm{d}t.$$

Now let us formulate the integral form of the cross-correlation function of shifted functions:

$$\begin{aligned} Q_{f,f_{sh}}(x,y) &= f(x,y) * f^*_{sh}(-x,-y) = f(x,y) * f(-x-x_0, -y-y_0) = \\ &= \int_{-\infty}^{\infty}\int_{-\infty}^{\infty} f(s,t)f(s-x-x_0, t-y-y_0)\mathrm{d}s\mathrm{d}t. \end{aligned}$$

And for $(x, y) = (-x_0, -y_0)$ we obtain

$$Q_{f,f_{sh}}(-x_0, -y_0) = \int_{-\infty}^{\infty}\int_{-\infty}^{\infty} f(s,t)f(s,t)\mathrm{d}s\mathrm{d}t = \int_{-\infty}^{\infty}\int_{-\infty}^{\infty} f^2(s,t)\mathrm{d}s\mathrm{d}t.$$

Then the previous inequality can be rewritten as

$$Q_{f,f_{sh}}(x, y) \leq Q_{f,f_{sh}}(-x_0, -y_0) \quad \forall (x, y) \in \mathbb{R}^2.$$

□

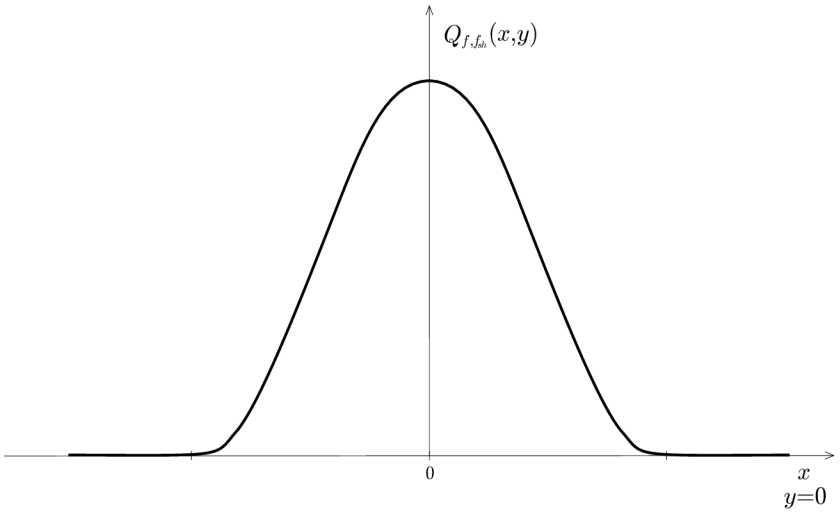


Figure 2.1: Typical shape of autocorrelation function showing clear global maximum

On the other hand to phase-correlation function, it is not so easy to find the shift using cross-correlation. The task is to find the global maximum (its coordinates) of the cross-correlation function and then to multiply it with $-1$. There would be an issue if the function had more than one global maximum. This case fortunately can not happen, because the cross-correlation function of an image with itself (autocorrelation function) has very specific shape shown in the Figure 2.1. The cross-correlation function of shifted images is just the shifted autocorrelation function.

**Theorem 2.30. (Cross-correlation function of functions with two shifted objects)** Let $f(x, y) \in \mathcal{L}(\mathbb{R}^2)$ continuous real and it has objects $f_1(x, y), f_2(x, y)$. Let $g(x, y)$ be function with shifted objects according to $f(x, y)$ by shift vectors $(x_1, y_1), (x_2, y_2)$ which are sufficiently different. Then the cross-correlation function of functions $f, g$ has local maxima $[-x_1, -y_1]$ and $[-x_2, -y_2]$.

*Proof.* It holds

$$\begin{aligned}
Q_{f,g}(x, y) &= f(x, y) * g(-x, -y) = \\
&= (f_1(x, y) + f_2(x, y)) \cdot (f_1(-x - x_1, -y - y_1) + f_2(-x - x_2, -y - y_2)) = \\
&= f_1(x, y) * f_1(-x - x_1, -y - y_1) + f_1(x, y) * f_2(-x - x_2, -y - y_2) + \\
&+ f_2(x, y) * f_1(-x - x_1, -y - y_1) + f_2(x, y) * f_2(-x - x_2, -y - y_2) = \\
&= Q_{f_1,f_{1,sh}} + Q_{f_2,f_{2,sh}} + Q_{f_1,f_{2,sh}} + Q_{f_2,f_{1,sh}},
\end{aligned}$$

which is summation of positive functions with sufficiently far global maxima. It means, that maxima are preserved as local maxima. □

We require the shift vectors to be sufficiently different for the maxima to stay maxima in summed function. If the maxima are to close, they will merge in one, or they could became even more close. Because of the very specific shape of autocorrelation function, there is no problem in existence of local maxima in the summed function. The global maximas in original functions are significant enough.

If the objects $f_1, f_2$ are not the same, there will not be formed another maxima, because they are not correlated. On the other hand, there will be formed two new maxima if $f_2(x, y) = f_1(x - x_0, y - y_0)$ (i.e. the objects are just shifted). The coordinates of the new maxima would be $[-x_0 - x_2, -y_0 - y_2], [x_0 - x_1, y_0 - y1]$, which can be easily proven analogically to proof of the Theorem 2.29. These maxima are comprising the mutual position of the objects and their shifts together.

**Theorem 2.31. (Cross-correlation function of fuctions with $n$ shifted objets)** Let $f(x, y) \in \mathcal{L}(\mathbb{R}^2)$ continuous real and it has objects $f_i(x, y)$, $i = 1, 2, ..., n$. Let $g(x, y)$ be function with shifted objects according to $f(x, y)$ by shift vectors $(x_i, y_i)$ which are sufficiently different. Then the cross-correlation function of functions $f, g$ has local maxima $[-x_i, -y_i]$. And it holds

$$Q_{f,g}(x, y) = \sum_{i=1}^{n} \sum_{j=1}^{n} Q_{f_i, f_{j,sh}}.$$

*Proof.* Proof can be derived as outward generalization of proof of the Theorem 2.30. □

# Chapter 3

# The discrete Fourier Transform

## 3.1 Digital image

At first, we need to define what do we mean by digital image to work with them. The digital image is two dimensional discrete representation of real-world scene that represents a momentary event from the three-dimensional spatial world which is created by a digital camera. The digital image like this contains an additive noise. It changes image we wanted to capture and we try to get rid of it in digital image processing. It is usually caused by increased temperature of camera sensor or some dust on the lens. To further image processing done in this thesis, we assume the image to be without additive noise. The images without additive noise can be also created in graphic programmes, but they are no longer real-world representations (i.e. photography). We will use them as testing images.

We will consider the image to be a two dimensional discrete function of the square shape in following chapters. That means that we will know the values of function only on integer coordinates. The values of an image are also consider to be integer, when we want to display it by some output displaying device. Yet, we will work with complex-valued (or real-valued) images in following chapter. This approach is more general and allows us to be more precise.

**Definition 3.1. (Digital gray-scale image)**[1] Let $R = \{0, 1, ..., N-1\}^2$, , $N \in \mathbb{N}$ and let $W = \{0, 1, ..., w-1\}$, $w \in \mathbb{N}$. Function

$$f(x, y) : R \longrightarrow W$$

is called a *digital gray-scale image*. Where $N$ is called the *image width* and the *image height*. Elements of $R$ are called *pixels* and value of $f$ in pixel $(x, y)$ is called the *pixel value*. The value of $w$ determines the image *dynamic range*. The dynamic range is $n$ *bits per pixel* (it is an $n$*-bit image*) if $w = 2^n$.

An image is usually defined to be rectangular, but it is sufficient for needs of this thesis for image to be square for phase correlation (or cross correlation) to work properly.

We usually use matrix to represent image and we call it *image matrix*. However there is no sense to use operation defined to matrices for image matrix, because it is just table of pixel values in coordinates $(x, y)$. Every operation applied to image matrix is meant to be applied on each pixel separately.

The dynamic range of the image is given by the memory representation of the image in computer. The $n$ determines, how much bits need to be used to save one pixel. We use

the dynamic range of this form to best use of the memory. Also the output displaying devices are made to display in classic dynamic range.

**Definition 3.2. (Digital color image)**[1] A *digital color image* is a triple of digital gray-scale images $(r, g, b)$ which are called the *red*, *green* and *blue color channels*.

For purposes of image registration we convert the digital color image into gray scale image. To do that we compute a convex combination of the red, green and blue color channels

$$f(x, y) = \text{Round}(c_r r(x, y) + c_g g(x, y) + c_b b(x, y)),$$

where $c_r, c_g, c_b \in \langle 0, 1\rangle$ and $c_r + c_g + c_b = 1$. The constants $c_r, c_g, c_b$ should be chosen to minimize the standard deviation of additive noise in image $f$. There is no rule for choosing constants that works for all images. For general images (taken without any color filters) we use assessment around

$$c_r = \frac{1}{9}, c_g = \frac{6}{9}, c_b = \frac{2}{9}.$$

**Definition 3.3. (Additive noise)**[1] Let $f$ be a digital gray-scale image representing an ideal image (containing no additive noise), let $n$ be a digital gray-scale image of the same size as $f$, whose pixel values are rounded independent realization of random variable $X$, which usually has normal distribution. Let

$$h(x, y) = \begin{cases} f(x, y) + n(x, y) & \text{if } 0 \leq f(x, y) + n(x, y) < w, \\ w - 1 & \text{if } f(x, y) + n(x, y) \geq w \end{cases}$$

then we say that image $h$ *contains additive noise*. Image $n$ is called *noise image*.

## 3.2 The Discrete Fourier transform and inverse Fourier transform

**Definition 3.4. (Discrete Fourier transform)**[8] Let $f\,(x, y) : \{0, 1, ..., N - 1\} \times \{0, 1, ..., N - 1\} = \{0, 1, ..., N - 1\}^2 \longrightarrow \mathbb{C}, N \in \mathbb{N}$. The *discrete Fourier transform* of function (image) $f(x, y)$ is function $\mathcal{D}\{f\}(\xi, \eta) = F(\xi, \eta) : \{0, 1, ..., N - 1\}^2 \to \mathbb{C}$ defined as

$$\mathcal{D}\{f\}(\xi, \eta) = F(\xi, \eta) = \sum_{x=0}^{N-1}\sum_{y=0}^{N-1} f(x, y)\mathrm{e}^{-\frac{2\pi i}{N}(x\xi+y\eta)}.$$

Function $F$ is also called the *Fourier spectrum* of function $f$.

**Definition 3.5. (Inverse discrete Fourier transform)**[8] Let function (image) $f(x, y)$ be a function $\{0, 1, ..., N - 1\}^2 \to \mathbb{C}, N \in \mathbb{N}$ and let $F(\xi, \eta)$ be its discrete Fourier transform. The *inverse discrete Fourier transform* of function $F(\xi, \eta)$ is function $\mathcal{D}^{-1}\{F\}(x, y) = g(x, y) : \{0, 1, ..., N - 1\}^2 \to \mathbb{C}$ defined as

$$\mathcal{D}^{-1}\{F\}(x, y) = \frac{1}{N^2}\sum_{\xi=0}^{N-1}\sum_{\eta=0}^{N-1} F(\xi, \eta)\mathrm{e}^{\frac{2\pi i}{N}(x\xi+y\eta)}.$$

**Theorem 3.6. (Fourier inversion theorem )**[1] Let $f(x, y)$ be a function (image) $\{0, 1, ..., N - 1\}^2 \to \mathbb{C}, N \in \mathbb{N}$ and let $F(\xi, \eta)$ be its discrete Fourier transform. Then the inverse discrete Fourier transform of function $F(\xi, \eta)$ is function $f(x, y)$, i.e.

$$\mathcal{D}^{-1}\{\mathcal{D}\{f(x, y)\}\} = f(x, y).$$

*Proof.* Proof taken from [1].

$$\begin{aligned}
\mathcal{D}^{-1}\{\mathcal{D}\{f(x,y)\}\} &= \frac{1}{N^2}\sum_{\xi=0}^{N-1}\sum_{\eta=0}^{N-1} F(\xi,\eta)\mathrm{e}^{\frac{2\pi\mathrm{i}}{N}(x\xi+y\eta)} = \\
&= \frac{1}{N^2}\sum_{\xi=0}^{N-1}\sum_{\eta=0}^{N-1}\sum_{s=0}^{N-1}\sum_{t=0}^{N-1} f(s,t)\mathrm{e}^{-\frac{2\pi\mathrm{i}}{N}(s\xi+t\eta)}\mathrm{e}^{\frac{2\pi\mathrm{i}}{N}(x\xi+y\eta)} = \\
&= \frac{1}{N^2}\sum_{s=0}^{N-1}\sum_{t=0}^{N-1} f(s,t)\sum_{\xi=0}^{N-1}\sum_{\eta=0}^{N-1}\mathrm{e}^{\xi\frac{2\pi\mathrm{i}}{N}(x-s)}\mathrm{e}^{\eta\frac{2\pi\mathrm{i}}{N}(y-t)} = \\
&= \frac{1}{N^2}\sum_{s=0}^{N-1}\sum_{t=0}^{N-1} f(s,t)\left(\sum_{\xi=0}^{N-1}\left(\mathrm{e}^{\frac{2\pi\mathrm{i}}{N}(x-s)}\right)^{\xi}\right)\left(\sum_{\eta=0}^{N-1}\left(\mathrm{e}^{\frac{2\pi\mathrm{i}}{N}(y-t)}\right)^{\eta}\right),
\end{aligned}$$

let us denote $g(s) = \sum_{\xi=0}^{N-1}(\mathrm{e}^{\frac{2\pi\mathrm{i}}{N}(x-s)})^{\xi}$ and $g(t) = \sum_{\eta=0}^{N-1}(\mathrm{e}^{\frac{2\pi\mathrm{i}}{N}(y-t)})^{\eta}$. $g(s)$ is finite geometrical series, therefore we can compute its sum. If $\mathrm{e}^{\frac{2\pi\mathrm{i}}{N}(x-s)} = 1$ (i.e. $x = s$), then $g(s) = N$ . Otherwise, $x - s \in \mathbb{Z} - \{0\}$ and

$$g(s) = \frac{1-\left(\mathrm{e}^{\frac{2\pi\mathrm{i}}{N}(x-s)}\right)^{N}}{1-\mathrm{e}^{\frac{2\pi\mathrm{i}}{N}(x-s)}} = \frac{1-\mathrm{e}^{2\pi\mathrm{i}(x-s)}}{1-\mathrm{e}^{\frac{2\pi\mathrm{i}}{N}(x-s)}} = \frac{1-1}{1-\mathrm{e}^{\frac{2\pi\mathrm{i}}{N}(x-s)}} = 0.$$

Similarly,

$$g(t) = \begin{cases} N & \text{if } y = t \\ 0 & \text{else.} \end{cases}$$

Therefore,

$$\mathcal{D}^{-1}\{\mathcal{D}\{f(x,y)\}\} = \frac{1}{N^2}f(x,y)\cdot N\cdot N = f(x,y).$$

□

On the contrary to the Fourier transform, the discrete Fourier transform always exists due to the fact that the summation is over a finite number of points. We also do not need to make restrictions to the functions as we need to in continuous case.

To further work with images (especially with shifted images) we need to define the periodized functions (images), so it would be possible to work with coordinates, which lay out of function domain.

**Definition 3.7. (Periodization of function and its Fourier spectrum )**[1] Let $f(x,y)$ be a function $\{0,1,...,N-1\}^2 \longrightarrow \mathbb{C}, N \in \mathbb{N}$ and let $F(\xi,\eta)$ be its Fourier spectrum. The *periodization of the Fourier spectrum* $F$ if function $\tilde{F}(\xi,\eta) : \mathbb{Z}^2 \longrightarrow \mathbb{C}$ defined as

$$\tilde{F}(\xi,\eta) = \sum_{x=0}^{N-1}\sum_{y=0}^{N-1} f(x,y)\mathrm{e}^{\frac{-2\pi\mathrm{i}}{N}(x\xi+y\eta)}.$$

The *periodization of function* $f$ is function $\tilde{f}(x,y) : \mathbb{Z}^2 \longrightarrow \mathbb{C}$ defined as

$$\tilde{f}(x,y) = \frac{1}{N^2}\sum_{\xi=0}^{N-1}\sum_{\eta=0}^{N-1} F(\xi,\eta)\mathrm{e}^{\frac{2\pi\mathrm{i}}{N}(x\xi+y\eta)}.$$

**Remark 3.8.** [1] For further usage of periodized functions let us remark some basic equalities. Let $f(x,y)$ be a function $\{0,1,...,N-1\}^2 \longrightarrow \mathbb{C}, N \in \mathbb{N}$. Then for every $(x,y),(\xi,\eta) \in \{0,1,...,N-1\}^2$ and $k,l \in \mathbb{Z}$ it holds

$$\begin{aligned} f(x,y) &= \tilde{f}(x+kN, y+lN), \\ F(\xi,\eta) &= \tilde{F}(\xi+kN, \eta+lN). \end{aligned}$$

In particular

$$\begin{aligned} \tilde{f}(x,y) = f(x,y), \qquad & \tilde{f}(-x,-y) = f(N-x, N-y), \\ \tilde{F}(\xi,\eta) = F(\xi,\eta), \qquad & \tilde{F}(-\xi,-\eta) = F(N-\xi, N-\eta). \end{aligned}$$

**Definition 3.9. (Discrete Fourier transform of periodized functions)**[1] Let $f(x,y)$ be function $\{0,1,...,N-1\}^2 \longrightarrow \mathbb{C}, N \in \mathbb{N}$. The discrete Fourier transform of the periodization of function $f, \tilde{f}(x,y) : \mathbb{Z}^2 \longrightarrow \mathbb{C}$ is function $\mathcal{D}\{\tilde{f}\}(\xi,\eta) = F(\xi,\eta) : \{0,1,...,N-1\}^2 \longrightarrow \mathbb{C}$ defined as

$$F(\xi,\eta) = \sum_{x=0}^{N-1}\sum_{y=0}^{N-1} = \tilde{f}(x,y)\mathrm{e}^{-\frac{2\pi\mathrm{i}}{N}(x\xi+y\eta)}.$$

**Definition 3.10. (Inverse discrete Fourier transform of periodized functions)**[1] Let $f(x,y)$ be a function $\{0,1,...,N-1\}^2 \longrightarrow \mathbb{C}, N \in \mathbb{N}$ and let $F(\xi,\eta)$ be its discrete Fourier transform with periodization $\tilde{F}(\xi,\eta) : \mathbb{Z}^2 \longrightarrow \mathbb{C}$. The inverse discrete Fourier transform of function $\tilde{F}(\xi,\eta)$ is function $\mathcal{D}^{-1}\{\tilde{F}\}(x,y) : \{0,1,...,N-1\}^2 \longrightarrow \mathbb{C}$ defined as

$$\mathcal{D}^{-1}\{\tilde{F}\}(x,y) = \frac{1}{N^2}\sum_{\xi=0}^{N-1}\sum_{\eta=0}^{N-1}\tilde{F}(\xi,\eta)\mathrm{e}^{\frac{2\pi\mathrm{i}}{N}(x\xi+y\eta)}.$$

**Corollary 3.11.** [1] Let $f(x,y)$ be a function $\{0,1,...,N-1\}^2 \longrightarrow \mathbb{C}, N \in \mathbb{N}$ with Fourier spectrum $F(\xi,\eta)$. For every $(x,y) \in \{0,1,...,N-1\}^2$, it holds:

$$\begin{aligned} \mathcal{D}\left\{f(x,y)\right\} &= \mathcal{D}\left\{\tilde{f}(x,y)\right\}, \\ \mathcal{D}^{-1}\left\{\mathcal{D}\left\{\tilde{f}(x,y)\right\}\right\} &= \mathcal{D}^{-1}\left\{\tilde{F}(\xi,\eta)\right\} = f(x,y). \end{aligned}$$

*Proof.* The claim is consequence of Definitions 3.9, 3.10 and Theorem 3.6. □

**Corollary 3.12.** [1] Let $f(x,y)$ be a function $\{0,1,...N-1\}^2 \longrightarrow \mathbb{C}, N \in \mathbb{N}$ with Fourier spectrum $F(\xi,\eta)$. For every $k,l \in \mathbb{Z}$ it holds:

$$\begin{aligned} \mathcal{D}\left\{f(x,y)\right\} &= \sum_{x=k}^{k+N-1}\sum_{y=l}^{l+N-1}\tilde{f}(x,y)\mathrm{e}^{-\frac{2\pi\mathrm{i}}{N}(x\xi+y\eta)}, \\ \mathcal{D}^{-1}\left\{F(\xi,\eta)\right\} &= \frac{1}{N^2}\sum_{\xi=k}^{k+N-1}\sum_{\eta=l}^{l+N-1}\tilde{F}(\xi,\eta)\mathrm{e}^{\frac{2\pi\mathrm{i}}{N}(x\xi+y\eta)}. \end{aligned}$$

*Proof.* The proof taken from [1]. The first claim is consequence of the fact, that both functions $\tilde{f}$ and $\mathrm{e}^{-\frac{2\pi\mathrm{i}}{N}(x\xi+y\eta)}$ for fixed $\xi,\eta \in \mathbb{Z}$ are $N$-periodic. The second claim is consequence of the fact that both functions $\tilde{F}$ and $\mathrm{e}^{\frac{2\pi\mathrm{i}}{N}(x\xi+y\eta)}$ for fixed $x,y \in \mathbb{Z}$ are $N$-periodic. □

## 3.3 Shift theorem for images

This section serves to introduce the concept of the shifted images and objects in the image. We will use the periodization of the image, because the shifts could lead out of the function domain. We will consider only integer shifts, because non-integer ones would lead out of the function domain. Even so, the mutual shifts finding method introduced in following chapter will compute even the non-integer shifts.

**Definition 3.13. (Shifted periodized images)** Let image $f(x,y)$ be a function $\{0,1,...,N-1\}^2 \longrightarrow \mathbb{C}, N \in \mathbb{N}$, let $\tilde{f}(x,y)$ be periodization of function $f$ and let $x_0, y_0 \in \mathbb{Z}$ be given numbers. The function $f_{sh}(x,y)$ is *shifted image* of image $f(x,y)$ by vector $(x_0,y_0)$ iff

$$f_{sh}(x,y) = \tilde{f}(x-x_0, y-y_0).$$

**Theorem 3.14. (Shift theorem for periodized images)**[1] Let image $f(x,y)$ be function $\{0,1,...,N-1\}^2 \longrightarrow \mathbb{C}, N \in \mathbb{N}$ and let $F(\xi,\eta)$ be its Fourier spectrum. Let $f_{sh}(x,y)$ be shifted image of image $f(x,y)$ and let $F_{sh}(\xi,\eta)$ be its Fourier spectrum. Then it holds

$$F_{sh}(\xi,\eta) = \mathrm{e}^{-\frac{2\pi\mathrm{i}}{N}(x_0\xi+y_0\eta)}F(\xi,\eta).$$

*Proof.* The following proof is shown in [1].

$$\begin{aligned}
F_{sh}(\xi,\eta) &= \sum_{x=0}^{N-1}\sum_{y=0}^{N-1} f_{sh}(x,y)\mathrm{e}^{-\frac{2\pi\mathrm{i}}{N}(x\xi+y\eta)} = \sum_{x=0}^{N-1}\sum_{y=0}^{N-1} \tilde{f}(x-x_0,y-y_0)\mathrm{e}^{-\frac{2\pi\mathrm{i}}{N}(x\xi+y\eta)} = \\
&= \left| \begin{array}{l} s = x-x_0 \\ t = y-y_0 \end{array} \right| = \sum_{s=-x_0}^{N-1-x_0}\sum_{t=-x_0}^{N-1-y_0} \tilde{f}(s,t)\mathrm{e}^{-\frac{2\pi\mathrm{i}}{N}(\xi(s+x_0)+\eta(t+y_0))} = \\
&= \mathrm{e}^{-\frac{2\pi\mathrm{i}}{N}(x_0\xi+y_0\eta)}\sum_{s=-x_0}^{N-1-x_0}\sum_{t=-x_0}^{N-1-y_0} \tilde{f}(s,t)\mathrm{e}^{-\frac{2\pi\mathrm{i}}{N}(s\xi+t\eta)} = \mathrm{e}^{-\frac{2\pi\mathrm{i}}{N}(x_0\xi+y_0\eta)}F(\xi,\eta).
\end{aligned}$$

The last equality is due to Corollary 3.11. □

**Definition 3.15. (Shifted images in greater scale)** Let $f_G(x,y)$ be an image (of greater scale) $\{0,1,...,N-1\}^2 \longrightarrow \mathbb{C}, N \in \mathbb{N}$. Let $x_0, y_0 \in \mathbb{Z}, k, l \in \mathbb{N}_0, M \in \mathbb{N}$ be given numbers such that

$$M < N,$$

$$\begin{array}{ll} k + x_0 \geq 0, & k + M + x_0 \geq N-1, \\ l + y_0 \geq 0, & l + M + y_0 \geq N-1. \end{array}$$

and let function $f$ be

$$f(x,y) = \begin{cases} f_G(x,y) & \text{if } (x,y) \in \{k,k+1,...,k+M-1\} \times \{l,l+1,...,l+M-1\} \\ 0 & \text{else.} \end{cases}$$

An image $g(x,y) : \{0,1,...,N-1\}^2 \longrightarrow \mathbb{C}$ is *shifted image* of image $f$ if it holds

$$g(x,y) = \begin{cases} f(x-x_0,y-y_0) & \text{if } \begin{array}{l} \max\{0,x_0\} \leq x \leq \min\{N-1, N-1+x_0\}, \\ \max\{0,y_0\} \leq y \leq \min\{N-1, N-1+y_0\}, \end{array} \\ 0 & \text{else.} \end{cases}$$

This is illustrated in [1] together with the definition.

**Theorem 3.16. (Shift Theorem)**[1] Let $f(x,y), g(x,y)$ be shifted images in greater scale and let $F(\xi,\eta), G(\xi,\eta)$ by their Fourier spectra. Then it holds

$$G(\xi,\eta) = \mathrm{e}^{-\frac{2\pi\mathrm{i}}{N}(x_0\xi+y_0\eta)}F(\xi,\eta).$$

*Proof.* Proof taken from [1].

$$\begin{aligned}
G(\xi,\eta) &= \sum_{x=0}^{N-1}\sum_{y=0}^{N-1} g(x,y)\mathrm{e}^{-\frac{2\pi\mathrm{i}}{N}(x\xi+y\eta)} = \sum_{x=k+x_0}^{k+M-1+x_0}\sum_{y=l+y_0}^{l+M-1+y_0} g(x,y)\mathrm{e}^{-\frac{2\pi\mathrm{i}}{N}(x\xi+y\eta)} = \\
&= \sum_{x=k+x_0}^{k+M-1+x_0}\sum_{y=l+y_0}^{l+M-1+y_0} f(x-x_0,y-y_0)\mathrm{e}^{-\frac{2\pi\mathrm{i}}{N}(x\xi+y\eta)} = \\
&= \left|\begin{array}{l} s = x-x_0 \\ t = y-y_0 \end{array}\right| = \sum_{s=k}^{k+M-1}\sum_{t=l}^{t+M-1} f(s,t)\mathrm{e}^{-\frac{2\pi\mathrm{i}}{N}(\xi(s+x_0)+\eta(t+y_0))} = \\
&= \mathrm{e}^{-\frac{2\pi\mathrm{i}}{N}(x_0\xi+y_0\eta)}\sum_{s=k}^{k+M-1}\sum_{t=l}^{l+M-1} f(s,t)\mathrm{e}^{-\frac{2\pi\mathrm{i}}{N}(s\xi+t\eta)} = \mathrm{e}^{-\frac{2\pi\mathrm{i}}{N}(x_0\xi+y_0\eta)}F(\xi,\eta).
\end{aligned}$$

□

We are introducing the concept of images cropped out of the greater scale because it is the easiest way to obtain testing image for finding mutual shift of shifted images. We are not using it further in this thesis though.

**Definition 3.17. (Multiple objects in image)** Let $n \in \mathbb{N}$ be given number, let images $f(x,y), f_i(x,y)$ be functions $\{0,1,...,N-1\}^2 \longrightarrow \mathbb{C}, N \in \mathbb{N}$ for each $i = 1,2,...,n$. Image $f(x,y)$ consists of $n$ objects $f_i(x,y)$ iff

$$f(x,y) = \sum_{i=1}^{n} f_i(x,y).$$

Introducing this concept of multiple objects in image could be problematic, if we were trying to create an image by the summation of multiple images. We know from the definition of the digital gray-scale image, that the image function can reach only non-negative values and the values are bounded. That could lead to summation of images, which result could overcome the dynamic range. Hence, the object image functions could take its values even from negative integer numbers. However, this is not the concept of creating image consisted of multiple objects but the formal description of an image, which is created in classical way.

**Definition 3.18. (Periodized image with shifted objects)** Let $f(x,y)$ be an image with $n$ shifted objects $f_i(x_i,y_i)$ and let $\tilde{f}_i(x,y)$ be their periodizations, let $x_i, y_i \in \mathbb{Z}$ be given numbers for each $i = 1,2,...,n$. Image $g(x,y) : \{0,1,...,N-1\}^2 \longrightarrow \mathbb{C}, N \in \mathbb{N}$ is *image with shifted objects* considering $f(x,y)$ iff

$$g(x,y) = \sum_{i=1}^{n} \tilde{f}_i(x-x_i,y-y_i).$$

To work with shifts, we need to consider periodized image again. Same as in continuous case, let us remark that each object $f_i(x,y)$ of image $f(x,y)$ is shifted in image $g(x,y)$. Therefore, we can say that objects $f_{i,sh}(x,y) = f_i(x-x_i, y-y_i)$ are shifted images of image functions (objects) $f_i(x,y)$ by vectors $(x_i, y_i)$. Also considering $n = 1$, we are obtaining the definition of the shifted image. So we can say, that the shifted function consist of only one object, which is shifted.

**Theorem 3.19. (Shift theorem for images with two objects)** Let $f(x,y)$ be a function with two objects ($n = 2$), let $F_1(\xi,\eta)$ and $F_2(\xi,\eta)$ be Fourier spectra of its objects $f_1(x,y), f_2(x,y)$. Let $g(x,y)$ be function with shifted objects considering $f(x,y)$ and let $G(\xi,\eta)$ be its Fourier spectrum. Then it holds

$$G(\xi,\eta) = F_1(\xi,\eta)\mathrm{e}^{-\frac{2\pi\mathrm{i}}{N}(x_1\xi+y_1\eta)} + F_2(\xi,\eta)\mathrm{e}^{-\frac{2\pi\mathrm{i}}{N}(x_2\xi+y_2\eta)}.$$

*Proof.*

$$\begin{aligned}
G(\xi,\eta) &= \sum_{x=0}^{N-1}\sum_{y=0}^{N-1} g(x,y)\mathrm{e}^{-\frac{2\pi\mathrm{i}}{N}(x\xi+y\eta)} = \\
&= \sum_{x=0}^{N-1}\sum_{y=0}^{N-1} (\tilde{f}_1(x-x_1, y-y_1) + \tilde{f}_2(x-x_2, y-y_2))\mathrm{e}^{-\frac{2\pi\mathrm{i}}{N}(x\xi+y\eta)} = \\
&= \sum_{x=0}^{N-1}\sum_{y=0}^{N-1} \tilde{f}_1(x-x_1, y-y_1)\mathrm{e}^{-\frac{2\pi\mathrm{i}}{N}(x\xi+y\eta)} + \\
&+ \sum_{x=0}^{N-1}\sum_{y=0}^{N-1} \tilde{f}_2(x-x_2, y-y_2)\mathrm{e}^{-\frac{2\pi\mathrm{i}}{N}(x\xi+y\eta)} = \\
&= \left|\begin{array}{ll} s = x - x_1 & x = s + x_1 \\ t = y - y_1 & y = t + y_1 \\ u = x - x_2 & x = u + x_2 \\ v = y - y_2 & y = v + y_2 \end{array}\right| = \sum_{s=-x_1}^{N-1-x_1}\sum_{t=-y_1}^{N-1-y_1} \tilde{f}_1(s,t)\mathrm{e}^{-\frac{2\pi\mathrm{i}}{N}((s+x_1)\xi+(t+y_1)\eta)} + \\
&+ \sum_{u=-x_2}^{N-1-x_2}\sum_{v=-y_2}^{N-1-y_2} \tilde{f}_2(u,v)\mathrm{e}^{-\frac{2\pi\mathrm{i}}{N}((u+x_2)\xi+(v+y_2)\eta)} = \\
&= \sum_{s=-x_1}^{N-1-x_1}\sum_{t=-y_1}^{N-1-y_1} \tilde{f}_1(s,t)\mathrm{e}^{-\frac{2\pi\mathrm{i}}{N}(s\xi+t\eta)}\mathrm{e}^{-\frac{2\pi\mathrm{i}}{N}(x_1\xi+y_1\eta)} + \\
&+ \sum_{u=-x_2}^{N-1-x_2}\sum_{v=-y_2}^{N-1-y_2} \tilde{f}_2(u,v)\mathrm{e}^{-\frac{2\pi\mathrm{i}}{N}(u\xi+v\eta)}\mathrm{e}^{-\frac{2\pi\mathrm{i}}{N}(x_2\xi+y_2\eta)} = \\
&= F_1(\xi,\eta)\mathrm{e}^{-\frac{2\pi\mathrm{i}}{N}(x_1\xi+y_1\eta)} + F_2(\xi,\eta)\mathrm{e}^{-\frac{2\pi\mathrm{i}}{N}(x_2\xi+y_2\eta)}.
\end{aligned}$$

□

**Theorem 3.20. (Shift theorem for images with $n$ objects)** Let $f(x,y)$ be an image with $n$ objects and let $F_i(\xi,\eta)$ be Fourier spectra of its objects $f_i(x,y)$ for each $i = 1, 2, ..., n$. Let $g(x,y)$ be an image with shifted objects considering $f(x,y)$ and let $G(\xi,\eta)$ be its Fourier spectrum. Then it holds

$$G(\xi,\eta) = \sum_{i=1}^{n} F_i(\xi,\eta)\mathrm{e}^{-\frac{2\pi\mathrm{i}}{N}(x_i\xi+y_i\eta)}.$$

*Proof.* Proof can be derived as outward generalization of proof of Theorem 3.19. □

## 3.4 Properties of discrete Fourier transform

As in continuous case, we are introducing some basic properties of the discrete Fourier transform which we are using in following sections.

**Theorem 3.21.** [8] Let image $f(x,y)$ be a function $\{0,1,...,N-1\}^2 \longrightarrow \mathbb{C}, N \in \mathbb{N}$ with Fourier spectrum $F(\xi,\eta)$ and let $\tilde{f},\tilde{F}$ be their periodizations. The discrete Fourier transform of function $f$ with reversed axes is function $F$ with reversed axes. The inverse discrete Fourier transform of function $F$ with reversed axes is function $f$ with reversed axes, i.e.

$$\begin{aligned}\mathcal{D}\left\{\tilde{f}(-x,-y)\right\} &= \tilde{F}(-\xi,-\eta) = F(N-\xi,N-\eta),\\ \mathcal{D}^{-1}\left\{\tilde{F}(-\xi,-\eta)\right\} &= \tilde{f}(-x,-y) = f(N-x,N-y).\end{aligned}$$

*Proof.* Proof taken from [1].

$$\begin{aligned}\mathcal{D}\left\{\tilde{f}(-x,-y)\right\} &= \sum_{x=0}^{N-1}\sum_{y=0}^{N-1}\tilde{f}(-x,-y)\mathrm{e}^{-\frac{2\pi\mathrm{i}}{N}(x\xi+y\eta)} = \left|\begin{array}{l} s=-x \\ t=-y \end{array}\right| =\\ &= \sum_{s=-N+1}^{0}\sum_{t=-N+1}^{0}\tilde{f}(s,t)\mathrm{e}^{-\frac{2\pi\mathrm{i}}{N}(-s\xi-t\eta)} = \tilde{F}(-\xi,-\eta).\end{aligned}$$

The last equality is due to the Corollary 3.12. The second claim is obtained from the first one by applying discrete inverse Fourier transform to its both sides. This step always works due to Theorem 3.6. □

**Theorem 3.22.** [4] Let image $f(x,y)$ be a function $\{0,1,...,N-1\}^2 \longrightarrow \mathbb{C}, N \in \mathbb{N}$ and let $F(\xi,\eta)$ be its Fourier spectrum. Then the Fourier transform of the complex conjugate of function $f$ is $\tilde{F^*}(-\xi,-\eta)$ i.e.

$$\mathcal{D}\left\{f^*(x,y)\right\} = \tilde{F^*}(-\xi,-\eta).$$

*Proof.* proof taken from [1].

$$\begin{aligned}\mathcal{D}\left\{f^*(x,y)\right\} &= \sum_{x=0}^{N-1}\sum_{y=0}^{N-1}f^*(x,y)\mathrm{e}^{-\frac{2\pi\mathrm{i}}{N}(x\xi+y\eta)} = \sum_{x=0}^{N-1}\sum_{y=0}^{N-1}f^*(x,y)\mathrm{e}^{\frac{2\pi\mathrm{i}}{N}(-x\xi-y\eta)} =\\ &= \left(\sum_{x=0}^{N-1}\sum_{y=0}^{N-1}f(x,y)\mathrm{e}^{-\frac{2\pi\mathrm{i}}{N}(-x\xi-y\eta)}\right)^* = \tilde{F^*}(-\xi,-\eta).\end{aligned}$$

□

**Theorem 3.23.** [1] Let $f(x,y)$ be a function $\{0,1,...,N-1\}^2 \longrightarrow \mathbb{C}, N \in \mathbb{N}$. Then it holds

(a) $\mathcal{D}\left\{\mathcal{D}\left\{f(x,y)\right\}\right\} = N^2\tilde{f}(-x,-y),$

(b) $\mathcal{D}^{-1}\left\{\mathcal{D}^{-1}\left\{f(x,y)\right\}\right\} = \frac{1}{N^2}\tilde{f}(-x,-y),$

(c) $$\mathcal{D}\left\{f(x,y)\right\} = N^2\mathcal{D}^{-1}\left\{\tilde{f}(-x,-y)\right\},$$

(d) $$\mathcal{D}^{-1}\left\{f(x,y)\right\} = \frac{1}{N^2}\mathcal{D}\left\{\tilde{f}(-x,-y)\right\}.$$

*Proof.* Proof taken from [1].

(a)

$$\begin{aligned}
\mathcal{D}\left\{\mathcal{D}\{f(x,y)\}\right\} &= \sum_{\xi=0}^{N-1}\sum_{\eta=0}^{N-1} F(\xi,\eta)\mathrm{e}^{-\frac{2\pi\mathrm{i}}{N}(x\xi+y\eta)} = \sum_{\xi=0}^{N-1}\sum_{\eta=0}^{N-1} F(\xi,\eta)\mathrm{e}^{\frac{2\pi\mathrm{i}}{N}(-x\xi-y\eta)} = \\
&= \left|\begin{array}{l}\sigma=-\xi\\ \tau=-\eta\end{array}\right| = \sum_{\sigma=-N+1}^{0}\sum_{\tau=-N+1}^{0} \tilde{F}(-\sigma,-\tau)\mathrm{e}^{\frac{2\pi\mathrm{i}}{N}(x\sigma+y\tau)} = \\
&= N^2\mathcal{D}^{-1}\left\{\mathcal{D}\{\tilde{f}(-x,-y)\}\right\} = N^2\tilde{f}(-x,-y).
\end{aligned}$$

(b)

$$\begin{aligned}
\mathcal{D}^{-1}\left\{\mathcal{D}^{-1}\{f(x,y)\}\right\} &= \frac{1}{N^2}\sum_{\xi=0}^{N-1}\sum_{\eta=0}^{N-1}\left(\frac{1}{N^2}\sum_{s=0}^{N-1}\sum_{t=0}^{N-1} f(s,t)\mathrm{e}^{\frac{2\pi\mathrm{i}}{N}(s\xi+t\eta)}\right)\mathrm{e}^{\frac{2\pi\mathrm{i}}{N}(x\xi+y\eta)} = \\
&= \frac{1}{N^4}\sum_{\xi=0}^{N-1}\sum_{\eta=0}^{N-1}\left(\sum_{s=0}^{N-1}\sum_{t=0}^{N-1} f(s,t)\mathrm{e}^{-\frac{2\pi\mathrm{i}}{N}(-s\xi-t\eta)}\right)\mathrm{e}^{\frac{2\pi\mathrm{i}}{N}(x\xi+y\eta)} = \\
&= \left|\begin{array}{l}u=-s\\ v=-t\end{array}\right| = \frac{1}{N^4}\sum_{\xi=0}^{N-1}\sum_{\eta=0}^{N-1}\left(\sum_{u=-N+1}^{0}\sum_{v=-N+1}^{0}\tilde{f}(-u,-v)\cdot\right. \\
&\quad \left.\cdot\,\mathrm{e}^{-\frac{2\pi\mathrm{i}}{N}(u\xi+v\eta)}\right)\mathrm{e}^{\frac{2\pi\mathrm{i}}{N}(x\xi+y\eta)} = \\
&= \frac{1}{N^2}\mathcal{D}^{-1}\left\{\mathcal{D}\{\tilde{f}(-x,-y)\}\right\} = \frac{1}{N^2}\tilde{f}(-x,-y).
\end{aligned}$$

(c) is obtained from (a) by applying the inverse discrete Fourier transform to both its sides

(d) is obtained from (b) by applying the discrete Fourier transform to both its sides, or by substituting $-x$ for $x$ and $-y$ for $y$ and dividing both sides by $N^2$.

□

**Theorem 3.24.** [1] Let image $f(x,y)$ be a function $\{0,1,...,N-1\}^2 \longrightarrow \mathbb{C}, N \in \mathbb{N}$ and have Fourier spectrum $F(\xi,\eta)$. The function $f$ is real, i.e. $f(x,y) = f^*(x,y)\ \forall(x,y) \in \{0,1,...,N-1\}^2$, iff $F(\xi,\eta) = \tilde{F}^*(-\xi,-\eta)$.

*Proof.* Proof taken from [1].

1. Let us suppose that $f$ is a real function. Then Theorem 3.22 implies that

$$F(\xi,\eta) = \mathcal{D}\{f(x,y)\} = \mathcal{D}\{f^*(x,y)\} = \tilde{F}^*(-\xi,-\eta).$$

2. Let us suppose that $F(\xi,\eta) = \tilde{F}^*(-\xi,-\eta)$. Then Theorem 3.22 and the Theorem 3.6 imply that

$$f(x,y) = \mathcal{D}^{-1}\{F(\xi,\eta)\} = \mathcal{D}^{-1}\{\tilde{F}^*(-\xi,-\eta)\} = \mathcal{D}^{-1}\left\{\mathcal{D}\{f^*(x,y)\}\right\} = f^*(x,y).$$

□

**Corollary 3.25.** [1] Let function $f(x,y) : \{0,1,...,N-1\}^2 \longrightarrow \mathbb{R}, N \in \mathbb{N}$. Let function $G(\xi,\eta) : \{0,1,...,N-1\}^2 \longrightarrow \mathbb{R}$ such that $G(\xi,\eta) = \tilde{G}(-\xi,-\eta)$. Then

$$\mathcal{D}^{-1}\{F(\xi,\eta)\cdot G(\xi,\eta)\}$$

is real.

*Proof.* Proof taken from [1]. According to Theorem 3.24 if $f$ is real, then

$$F(\xi,\eta) = \tilde{F}^*(-\xi,-\eta).$$

By multiplying the equality by $G$, we obtain

$$F(\xi,\eta)\cdot G(\xi,\eta) = \tilde{F}^*(-\xi,-\eta)\cdot\tilde{G}(-\xi,-\eta) = \left(\tilde{F}(-\xi,-\eta)\cdot\tilde{G}(-\xi,-\eta)\right)^*.$$

Then again according to Theorem 3.24

$$\mathcal{D}^{-1}\{F(\xi,\eta)\cdot G(\xi,\eta)\}$$

is real. □

## 3.5 Discrete periodic convolution

The discrete periodic convolution is the most used tool in image processing. It is usually used with much smaller kernel. We will also use the discrete periodic convolution to reduce complexity of the computations.

**Definition 3.26. (Discrete periodic convolution)**[8] Let images $f(x,y), g(x,y)$ be functions $\{0,1,...,N-1\}^2 \longrightarrow \mathbb{C}, N \in \mathbb{N}$. The *discrete periodic convolution* of functions $f, g$ is function $\{0,1,...,N-1\}^2 \longrightarrow \mathbb{C}$ defined as

$$h(x,y) = f(x,y) * g(x,y) = \sum_{s=0}^{N-1}\sum_{t=0}^{N-1} f(s,t)\tilde{g}(x-s,y-t).$$

**Theorem 3.27.** [1] Let images $f(x,y), g(x,y)$ be functions $\{0,1,...,N-1\}^2 \longrightarrow \mathbb{C}, N \in \mathbb{N}$ and have Fourier spectra $F(\xi,\eta), G(\xi,\eta)$. Then

$$\mathcal{D}\{f(x,y) * g(x,y)\} = F(\xi,\eta)\cdot G(\xi,\eta).$$

*Proof.* Similar proof can be found in [8]. Let $h(x,y) = f(x,y) * g(x,y)$, then

$$\begin{aligned}
\mathcal{D}\{h(x,y)\} &= \sum_{x=0}^{N-1}\sum_{y=0}^{N-1}\left(\sum_{s=0}^{N-1}\sum_{t=0}^{N-1} f(s,t)\tilde{g}(x-s,y-t)\right)\mathrm{e}^{-\frac{2\pi\mathrm{i}}{N}(x\xi+y\eta)} = \\
&= \sum_{x=0}^{N-1}\sum_{y=0}^{N-1} f(s,t)\sum_{s=0}^{N-1}\sum_{t=0}^{N-1}\tilde{g}(x-s,y-t)\mathrm{e}^{-\frac{2\pi\mathrm{i}}{N}(x\xi+y\eta)} = \left|\begin{array}{l} p = x-s \\ q = y-t \end{array}\right| = \\
&= \sum_{x=0}^{N-1}\sum_{y=0}^{N-1} f(s,t)\sum_{p=-s}^{N-1-s}\sum_{q=-t}^{N-1-t}\tilde{g}(p,q)\mathrm{e}^{-\frac{2\pi\mathrm{i}}{N}((p+s)\xi+(q+t)\eta)} = \\
&= \sum_{x=0}^{N-1}\sum_{y=0}^{N-1} f(s,t)\mathrm{e}^{-\frac{2\pi\mathrm{i}}{N}(s\xi+t\eta)}\sum_{p=-s}^{N-1-s}\sum_{q=-t}^{N-1-t}\tilde{g}(p,q)\mathrm{e}^{-\frac{2\pi\mathrm{i}}{N}(p\xi+q\eta)} = \\
&= F(\xi,\eta)\cdot G(\xi,\eta).
\end{aligned}$$

□

**Theorem 3.28.** [4] Let images $f(x,y), g(x,y)$ be functions $\{0,1,...,N-1\}^2 \longrightarrow \mathbb{C}, N \in \mathbb{N}$ and have Fourier spectra $F(\xi,\eta), G(\xi,\eta)$. Then

$$\mathcal{D}\{f(x,y)\cdot g(x,y)\} = \frac{1}{N^2}F(\xi,\eta) * G(\xi,\eta).$$

*Proof.* Proof taken from [1]. Let $h(x,y) = f(x,y) * g(x,y)$. Using the Fourier Inversion Theorem 3.6 we can compute $\mathcal{D}\{h(x,y)\}$ as

$$\begin{aligned}
\mathcal{D}\{h(x,y)\} &= \sum_{x=0}^{N-1}\sum_{y=0}^{N-1} f(x,y)g(x,y)\mathrm{e}^{-\frac{2\pi\mathrm{i}}{N}(x\xi+y\eta)} = \\
&= \sum_{x=0}^{N-1}\sum_{y=0}^{N-1}\left(\frac{1}{N^2}\sum_{\sigma=0}^{N-1}\sum_{\tau=0}^{N-1} F(\sigma,\tau)\mathrm{e}^{\frac{2\pi\mathrm{i}}{N}(x\sigma+y\tau)}\right) g(x,y)\mathrm{e}^{-\frac{2\pi\mathrm{i}}{N}(x\xi+y\eta)} = \\
&= \frac{1}{N^2}\sum_{\sigma=0}^{N-1}\sum_{\tau=0}^{N-1} F(\sigma,\tau)\sum_{x=0}^{N-1}\sum_{y=0}^{N-1} g(x,y)\mathrm{e}^{-\frac{2\pi\mathrm{i}}{N}(x(\xi-\sigma)+y(\eta-\tau))} = \\
&= \frac{1}{N^2}\sum_{\sigma=0}^{N-1}\sum_{\tau=0}^{N-1} F(\sigma,\tau)\tilde{G}(\xi-\sigma,\eta-\tau) = \frac{1}{N^2}F(\xi,\eta) * G(\xi,\eta).
\end{aligned}$$

□

**Theorem 3.29. (Distributivity of discrete periodic convolution)** Let images $f(x,y)$, $g(x,y), h(x,y)$ be functions $\{0,1,...N-1\}^2 \longrightarrow \mathbb{C}, N \in \mathbb{N}$. Then it holds

$$f(x,y) * (g(x,y) + h(x,y)) = f(x,y) * g(x,y) + f(x,y) * h(x,y).$$

*Proof.* Let us denote $k(x,y) = g(x,y) + h(x,y)$. Then

$$\begin{aligned} f(x,y) * (g(x,y) + h(x,y)) &= f(x,y) * k(x,y) = \sum_{s=0}^{N-1}\sum_{t=0}^{N-1} f(s,t)\tilde{k}(x-s,y-t) = \\ &= \sum_{t=0}^{N-1} f(s,t)(\tilde{g}(x-s,y-t) + \tilde{h}(x-s,y-t)) = \\ &= \sum_{t=0}^{N-1} f(s,t)\tilde{g}(x-s,y-t) + \sum_{t=0}^{N-1} f(s,t)\tilde{h}(x-s,y-t)) = \\ &= f(x,y) * g(x,y) + f(x,y) * h(x,y). \end{aligned}$$

□

## 3.6 Cross correlation, phase correlation

The concept of cross correlation and phase correlation is very similar to the continuous case, it brings the same problems with the same solutions.

**Definition 3.30. (Cross-power spectrum, normalized cross-power spectrum)**[3] Let images $f(x,y), g(x,y)$ be functions $\{0,1,...,N-1\}^2 \longrightarrow \mathbb{C}, N \in \mathbb{N}$ and have Fourier spectra $F(\xi,\eta), G(\xi,\eta)$. The *cross-power spectrum* of functions $f, g$ is function $C_{f,g}(\xi,\eta) : \{0,1,..,N-1\}^2 \longrightarrow \mathbb{C}$ defined as

$$C_{f,g}(\xi,\eta) = F(\xi,\eta) \cdot G^*(\xi,\eta).$$

The *normalized cross-power spectrum* of functions $f, g$ is function $Z_{f,g}(\xi,\eta) : \{0,1,...,N-1\}^2 \longrightarrow \mathbb{C}$ defined by

$$Z_{f,g}(\xi,\eta) = \frac{F(\xi,\eta) \cdot G^*(\xi,\eta)}{|F(\xi,\eta) \cdot G(\xi,\eta)|}.$$

**Definition 3.31. (Cross-correlation function, phase-correlation function)**[1] Let functions $F(x,y), G(x,y) : \{0,1,...,N-1\}^2 \longrightarrow \mathbb{C}, N \in \mathbb{N}$ have Fourier spectra $F(\xi,\eta)$, $G(\xi,\eta)$. The function $Q_{f,g}(x,y) : \{0,1,...,N-1\}^2 \longrightarrow \mathbb{C}$ defined as

$$Q_{f,g}(x,y) = \mathcal{D}^{-1}\{C_{f,g}(\xi,\eta)\} = \mathcal{D}^{-1}\{F(\xi,\eta) \cdot G^*(\xi,\eta)\}$$

is called *cross-correlation function* of functions $f, g$. Function $P_{f,g}(x,y) : \{0,1,...,N-1\}^2 \longrightarrow \mathbb{C}$ defined as

$$P_{f,g}(x,y) = \mathcal{D}^{-1}\{Z_{f,g}(\xi,\eta)\} = \mathcal{D}^{-1}\left\{\frac{F(\xi,\eta) \cdot G^*(\xi,\eta)}{|F(\xi,\eta) \cdot G(\xi,\eta)|}\right\}$$

is called *phase-correlation function* of functions $f, g$.

**Theorem 3.32. (Cross-correlation function for real functions)**[1] Let $f(x,y), g(x,y)$ be functions $\{0,1,...,N-1\}^2 \longrightarrow \mathbb{R}, N \in \mathbb{N}$ (real functions) and have Fourier spectra $F(\xi,\eta), G(\xi,\eta)$. Then the cross-correlation function of these function is real.

*Proof.* Proof taken from [1]. Using Theorems 3.6, 3.22 we obtain

$$\begin{aligned} Q_{f,g}(x,y) &= \mathcal{D}^{-1}\{F(\xi,\eta) \cdot G^*(\xi,\eta)\} = \mathcal{D}^{-1}\left\{\mathcal{D}\{f(x,y)\} \cdot \mathcal{D}\{\tilde{g^*}(-x,-y)\}\right\} = \\ &= \mathcal{D}^{-1}\left\{\mathcal{D}\{f(x,y) * \tilde{g^*}(-x,-y)\}\right\} = f(x,y) * \tilde{g^*}(-x,-y) = \\ &= f(x,y) * \tilde{g}(-x,-y), \end{aligned}$$

which is a real function. □

**Remark 3.33.** Noticeably, the cross-correlation function can be transformed to convolution as follows:

$$Q_{f,g}(x,y) = f(x,y) * g^*(-x,-y) = f(x,y) * g(-x,-y),$$

where $f(x,y), g(x,y) \in \mathcal{L}(\mathbb{R}^2)$ continuous real. This matter of fact is often used to reduce complexity of the computations. It will also be used as useful property of cross-correlation function in some of following proves.

**Definition 3.34. (Discrete impulse function)**[1] Let $d(x,y)$ be a function defined on $\{0,1,...,N-1\}^2$ as

$$d(x,y) = \begin{cases} 1 & \text{if } (x,y) = (0,0), \\ 0 & \text{else.} \end{cases}$$

function $d$ is called *discrete impulse function.*

For the purposes of finding mutual shifts, we need to consider the cross-power spectrum, cross-correlation function, normalized cross-power spectrum and phase correlation function to be periodized. We assume the periodization of these functions because we need to obtain negative coordinates for the positive shifts (see following theorems). However, this will lead to existence of periodized maxima too.

**Theorem 3.35. (Phase-correlation function of shifted images)**[1] Let image $f(x,y)$ be a function $\{0,1,...,N-1\}^2 \longrightarrow \mathbb{C}, N \in \mathbb{N}$ and let $F(\xi,\eta)$ be its Fourier spectrum. Let us consider $f_{sh}(x,y)$ to be a shifted image (see Definition 3.13) of $f(x,y)$ and let $F_{sh}(\xi,\eta)$ be its Fourier spectrum. Then the phase-correlation function of functions $f, f_{sh}$ is the discrete impulse function shifted by $(-x_0,-y_0)$

$$P_{f,f_{sh}}(x,y) = \tilde{d}(x+x_0, y+y_0).$$

*Proof.* Proof taken from [1]. Shift Theorem 3.14 implies that

$$Z_{f,f_{sh}}(\xi,\eta) = \frac{F(\xi,\eta)\cdot F^*(\xi,\eta)\left(\mathrm{e}^{-\frac{2\pi\mathrm{i}}{N}(x_0\xi+y_0\eta)}\right)^*}{\left|F(\xi,\eta)\cdot F(\xi,\eta)\mathrm{e}^{-\frac{2\pi\mathrm{i}}{N}(x_0\xi+y_0\eta)}\right|} = \mathrm{e}^{\frac{2\pi\mathrm{i}}{N}(x_0\xi+y_0\eta)}.$$

Further, according to the Theorem 3.23 (d) we can write

$$\begin{aligned}
\mathcal{D}^{-1}\{Z_{f,f_{sh}}(\xi,\eta)\} &= \frac{1}{N^2}\mathcal{D}\left\{\tilde{Z}_{f,f_{sh}}(-\xi,-\eta)\right\} = \frac{1}{N^2}\mathcal{D}\left\{\mathrm{e}^{\frac{2\pi\mathrm{i}}{N}(-x_0\xi-y_0\eta)}\right\} = \\
&= \frac{1}{N^2}\sum_{\xi=0}^{N-1}\sum_{\eta=0}^{N-1}\mathrm{e}^{-\frac{2\pi\mathrm{i}}{N}(x_0\xi+y_0\eta)}\mathrm{e}^{-\frac{2\pi\mathrm{i}}{N}(x\xi+y\eta)} = \\
&= \frac{1}{N^2}\left(\sum_{\xi=0}^{N-1}\mathrm{e}^{-\frac{2\pi\mathrm{i}}{N}\xi(x+x_0)}\right)\left(\sum_{\eta=0}^{N-1}\mathrm{e}^{-\frac{2\pi\mathrm{i}}{N}\eta(y+y_0)}\right) = \\
&= \frac{1}{N^2}\left(\sum_{\xi=0}^{N-1}\left(\mathrm{e}^{-\frac{2\pi\mathrm{i}}{N}(x+x_0)}\right)^{\xi}\right)\left(\sum_{\eta=0}^{N-1}\left(\mathrm{e}^{-\frac{2\pi\mathrm{i}}{N}(y+y_0)}\right)^{\eta}\right).
\end{aligned}$$

Similarly to the proof of the Fourier Inversion Theorem 3.6, let us denote $g(x) = \sum_{\xi=0}^{N-1}\left(\mathrm{e}^{-\frac{2\pi\mathrm{i}}{N}(x+x_0)}\right)^{\xi}$ and $g(y) = \sum_{\eta=0}^{N-1}\left(\mathrm{e}^{-\frac{2\pi\mathrm{i}}{N}(y+y_0)}\right)^{\eta}$. Where both functions $g(x)$ and $g(y)$ are

finite geometrical series. If $x = -x_0 + kN$ ($k$ is arbitrary integer number), $g(x) = N$ since all elements of the series are equal to 1. Otherwise

$$g(x) = \frac{1 - \left(\mathrm{e}^{-\frac{2\pi\mathrm{i}}{N}(x+x_0)}\right)^N}{1 - \mathrm{e}^{-\frac{2\pi\mathrm{i}}{N}(x+x_0)}} = \frac{1 - \mathrm{e}^{-2\pi\mathrm{i}(x+x_0)}}{1 - \mathrm{e}^{-\frac{2\pi\mathrm{i}}{N}(x+x_0)}} = \frac{1-1}{1 - \mathrm{e}^{-\frac{2\pi\mathrm{i}}{N}(x+x_0)}} = 0.$$

Analogically,

$$g(y) = \begin{cases} N & \text{if } y = -y_0 + lN,\ l \in \mathbb{Z}, \\ 0 & \text{else.} \end{cases}$$

Hence,

$$\begin{aligned} P_{f,g}(x,y) &= \mathcal{D}^{-1}\{Z_{f,g}(\xi,\eta)\} = \begin{cases} 1 & \text{if } (x,y) = (-x_0 + kN, -y_0 + lN) \\ & \text{for some } k,l \in \mathbb{Z}, \\ 0 & \text{else} \end{cases} \\ &= \tilde{d}(x + x_0, y + y_0). \end{aligned}$$

□

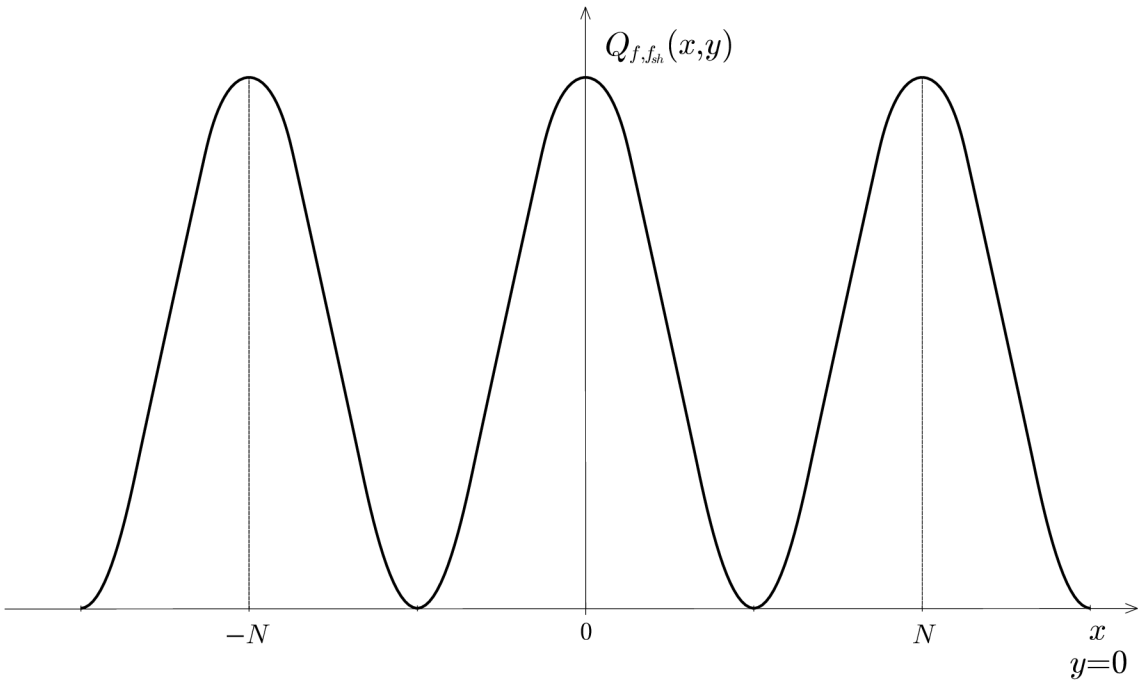


Figure 3.1: Typical shape of discrete autocorrelation function showing clear periodic global maxima

On the contrary to continuous case, there is more than one global maxima. However, we know, that their location is $N$-periodic. Which was proven. The shape of discrete autocorrelation function can be seen in Figure 3.1.

**Theorem 3.36. (Cross-correlation function of shifted images)** Let image $f(x,y)$ be a function $\{0,1,...,N-1\}^2 \longrightarrow \mathbb{R}, N \in \mathbb{N}$ and let us consider $f_{sh}(x,y)$ to be a shifted image (see Definition 3.13) of $f(x,y)$. Then the cross-correlation function of functions $f, f_{sh}$ has its global maxima in $[-x_0 + kN, -y_0 + lN]$, where $k,l \in \mathbb{Z}$ i.e.

$$Q_{f,f_{sh}}(x,y) \leq Q_{f,f_{sh}}(-x_0 + kN, -y_0 + lN) \quad \forall (x,y) \in \mathbb{R}^2.$$

*Proof.* Let us begin with equality

$$\begin{aligned}&\Big(f(s,t)-\tilde{f}(s-x-x_0,t-y-y_0)\Big)^2=\\ =\;& f^2(s,t)-2f(s,t)\tilde{f}(s-x-x_0,t-y-y_0)+\tilde{f}^2(s-x-x_0,t-y-y_0).\end{aligned}$$

By summation of both sides we obtain

$$\begin{aligned}&\sum_{s=0}^{N-1}\sum_{t=0}^{N-1}\Big(f(s,t)-\tilde{f}(s-x-x_0,t-y-y_0)\Big)^2=\sum_{s=0}^{N-1}\sum_{t=0}^{N-1}f^2(s,t)-\\ -\;& 2\sum_{s=0}^{N-1}\sum_{t=0}^{N-1}f(s,t)\tilde{f}(s-x-x_0,t-y-y_0)+\sum_{s=0}^{N-1}\sum_{t=0}^{N-1}\tilde{f}^2(s-x-x_0,t-y-y_0).\end{aligned}$$

Due to $2\pi$-periodicity of $\tilde{f}(x,y)$ we can write

$$\sum_{s=0}^{N-1}\sum_{t=0}^{N-1}\tilde{f}^2(s-x-x_0,t-y-y_0)=\sum_{s=0}^{N-1}\sum_{t=0}^{N-1}f^2(s,t).$$

Using this equality we obtain

$$\begin{aligned}&\sum_{s=0}^{N-1}\sum_{t=0}^{N-1}f(s,t)\tilde{f}(s-x-x_0,t-y-y_0)=\\ =\;&\sum_{s=0}^{N-1}\sum_{t=0}^{N-1}f^2(s,t)-\frac{1}{2}\sum_{s=0}^{N-1}\sum_{t=0}^{N-1}\Big(f(s,t)-\tilde{f}(s-x-x_0,t-y-y_0)\Big)^2.\end{aligned}$$

Since the last sum is finite and its members are non-negative, we can write

$$\sum_{s=0}^{N-1}\sum_{t=0}^{N-1}f(s,t)\tilde{f}(s-x-x_0,t-y-y_0)\le\sum_{s=0}^{N-1}\sum_{t=0}^{N-1}f^2(s,t).$$

Now let us formulate the summation form of the cross-correlation function of shifted functions:

$$\begin{aligned}Q_{f,f_{sh}}(x,y)&=f(x,y)*f^*_{sh}(-x,-y)=f(x,y)*\tilde{f}(-x-x_0,-y-y_0)=\\ &=\sum_{s=0}^{N-1}\sum_{t=0}^{N-1}f(s,t)\tilde{f}(s-x-x_0,t-y-y_0).\end{aligned}$$

And for $(x,y)=(-x_0+kN,-y_0+lN)$ we obtain

$$Q_{f,f_{sh}}(-x_0+kN,-y_0+lN)=\sum_{s=0}^{N-1}\sum_{t=0}^{N-1}f(s,t)\tilde{f}(s,t)=\sum_{s=0}^{N-1}\sum_{t=0}^{N-1}f^2(s,t).$$

Then the previous inequality can be rewritten as

$$Q_{f,f_{sh}}(x,y)\le Q_{f,f_{sh}}(-x_0+kN,-y_0+lN)\quad\forall(x,y)\in\mathbb{R}^2.$$

□

**Theorem 3.37. (Cross-correlation function of images with two shifted objects)** Let image $f(x,y)$ be a function $\{0,1,...,N-1\}^2 \longrightarrow \mathbb{R}, N \in \mathbb{N}$ and let it have objects $f_1(x,y), f_2(x,y)$ (see Definition 3.18 of image with shifted objects). Let $g(x,y)$ be an image with shifted objects according to $f(x,y)$ by shift vectors $(x_1,y_1),(x_2,y_2)$ which are sufficiently different. Then the cross-correlation function of functions $f,g$ has local maxima $[-x_1+k_1N,-y_1+l_1N]$ and $[-x_2+k_2N,-y_2+l_2N]$ where $k_1,k_2,l_1,l_2 \in \mathbb{N}$.

*Proof.* It holds

$$\begin{aligned} Q_{f,g}(x,y) &= f(x,y) * \tilde{g}(-x,-y) = \\ &= (f_1(x,y)+f_2(x,y)) \cdot (\tilde{f_1}(-x-x_1,-y-y_1)+\tilde{f_2}(-x-x_2,-y-y_2)) = \\ &= f_1(x,y) * \tilde{f_1}(-x-x_1,-y-y_1) + f_1(x,y) * \tilde{f_2}(-x-x_2,-y-y_2) + \\ &+ f_2(x,y) * \tilde{f_1}(-x-x_1,-y-y_1) + \tilde{f_2}(x,y) * \tilde{f_2}(-x-x_2,-y-y_2) = \\ &= Q_{f_1,f_{1,sh}} + Q_{f_2,f_{2,sh}} + Q_{f_1,f_{2,sh}} + Q_{f_2,f_{1,sh}}, \end{aligned}$$

which is summation of positive functions with sufficiently far global maxima. It means, that maxima are preserved as local maxima. □

**Theorem 3.38. (Cross-correlation function of functions with $n$ shifted objects)** Let image $f(x,y)$ be a function $\{0,1,...,N-1\}^2 \longrightarrow \mathbb{R}, N \in \mathbb{N}$ and let it have objects $f_i(x,y), i = 1,2,...,n$. Let $g(x,y)$ be an image with shifted objects according to $f(x,y)$ by shift vectors $(x_i,y_i)$ which are sufficiently different. Then the cross-correlation function of functions $f,g$ has local maxima $[-x_i+k_iN,-y_i+l_iN]$ . And it holds

$$Q_{f,g}(x,y) = \sum_{i=1}^{n}\sum_{j=1}^{n} Q_{f_i,f_{j,sh}}.$$

*Proof.* The proof can be obtained as outward generalization of proof of Theorem 3.37. □

# Chapter 4

# Implementation

We will focus on implementation of the previously introduced mathematical conclusions in this chapter. In first three sections, we will establish the basic form of input images for the algorithm to work properly. Next, we will introduce the algorithm for computing the shifts of shifted images and the sub-pixel precision of finding those shifts. At last, we will consider images containing multiple objects and computing the shifts of the objects. We are considering Finding the shifts of shifted images at first, because the algorithm is similar to Following of multiple objects movement to this point. It is also more showing. The next section is devoted to further adjustment of the previous algorithm for purposes of finding multiple shifts. And we are testing the precision of the algorithm in last section.

For purposes of this thesis, we will consider idealized testing images (i.e. images without any noise). That does not mean, that the algorithm does not work for non-idealized images taken by some camera. The following adjustments of the image will deal with most of the problems, which will be shortly mentioned.

All the theoretical background except the last section is drawn from [1] if not said otherwise.

As introduced in Chapter 3, the digital gray-scale image has integer values. All the spectra computed as defined in the Chapter 3 have non-integer values on the other hand. To visualize the spectra, we consider them to be digital image too. This causes no problem, because the cross-correlation function of real functions is also real (as proven in Corollary 3.25). Thus, we transform the values to fit into fitting dynamic range and round them. We also display all the spectra in logarithmic brightness scale to better see the non-zero values.

## 4.1 Input images

At first, let us discus the size of the input gray-scale image. Generally the $N$ can be arbitrary. However, for speeding up the Fast Fourier Transform algorithm [2] used for computing the discrete Fourier Transform, we need the $N$ to be composite number. If $N$ is a prime number, the number of elementary operations (a multiplication and addition of two complex numbers) is $N^2$. If $N = N_1 N_2 ... N_k$, $N_\iota \in \mathbb{N}, \forall \iota = 1, 2, ..., k$ then the number of operations needed is $N \sum_{\iota=1}^{k} N_i$. In particular, for $N = 2^k$ there is $2kN = 2N \log_2 N$ elementary operations required. Therefore, we will use $N$'s which are divisible by higher power of 2, at least 16, better 256 or higher, and which are not divisible by a high prime number.

If we are working with images which are smaller than $N \times N$, we center the image inside

the $N \times N$ square image and surround it by black area. Let us assume that image $f$ has width $\mu$ and height $\nu$. Let $N \in \mathbb{N}$ be previously discussed form such that $\mu \leq N, \nu \leq N$. Then we create image $f_c$ from image $f$ by

$$f_c(x,y) = \begin{cases} f(x-\mu_0, y-\nu_0) & \text{if } \mu_0 \leq x \leq \mu_0 + \mu - 1,\ \nu_0 \leq y \leq \nu_0 + \nu - 1 \\ 0 & \text{else,} \end{cases}$$

where $\mu_0 = \left\lfloor \frac{N-\mu}{2} \right\rfloor, \nu_0 = \left\lfloor \frac{N-\nu}{2} \right\rfloor$. As shown in [1].

## 4.2 Window function

The discrete Fourier transform works either with periodic images or makes them periodic (see Definition 3.7). And in general case, an image does not have the same values on the edges and by periodizing an image we obtain image with great jumps in values on the+previous edges. They often lead to incorrect results. Therefore, it is necessary to ensure that the edges are smoothed out. This is done by multiplying the image by suitable function so called window function. Commonly used window functions are the Gaussian and the Hanning window functions. They both are zero or almost zero on the edges and one on the majority of image interior.

**Definition 4.1. (Gaussian window function)**[1] Let sets

$$\begin{aligned} A &= \langle -a, a\rangle \times \langle -b, b\rangle, \qquad a, b \in \mathbb{R}_0^+, \\ B &= \{(x,y); x^2 + y^2 \leq r^2\}, \qquad r \in \mathbb{R}_0^+. \end{aligned}$$

Let $\sigma \in \mathbb{R}^+$ be a given number. Let $\rho(X, A)$ be the distance of the point $X = (x, y)$ from set $A$, i.e

$$\rho(X, A) = \inf\{d \in \mathbb{R}, d = \rho(X, Y), Y \in A\},$$

where $\rho(X, Y)$ is the Euclidean metric. Then function

$$w_{GR}(x,y) = \mathrm{e}^{-\frac{\rho^2(X,A)}{\sigma^2}}$$

is called the *rectangular Gaussian window function.* Function

$$w_{GC}(x,y) = \mathrm{e}^{-\frac{\rho^2(X,B)}{\sigma^2}}$$

is called the *circular Gaussian window function.*

**Definition 4.2. (Hanning window function)**[1] Let sets $A, B$ and metric $\rho$ be same as in previous definition. Then function

$$w_{HR}(x,y) = \begin{cases} \frac{1}{2}\left(1 + \cos\frac{\pi\rho(X,A)}{\sigma}\right) & \text{if } \rho(X,A) \leq \sigma, \\ 0 & \text{if } \rho(X,A) > \sigma \end{cases}$$

is called the *rectangular Hanning window function.* Function

$$w_{HC}(x,y) = \begin{cases} \frac{1}{2}\left(1 + \cos\frac{\pi\rho(X,B)}{\sigma}\right) & \text{if } \rho(X,B) \leq \sigma, \\ 0 & \text{if } \rho(X,B) > \sigma \end{cases}$$

is called the *circular Hanning window function.*

The window functions are defined symmetrical with center in $[0, 0]$, applied to images they need to be shifted by $\left(\frac{1}{2}, \frac{1}{2}\right)$, i.e. the image $f$ is multiplied by a window function $w\left(x - \frac{N}{2}, y - \frac{N}{2}\right)$.

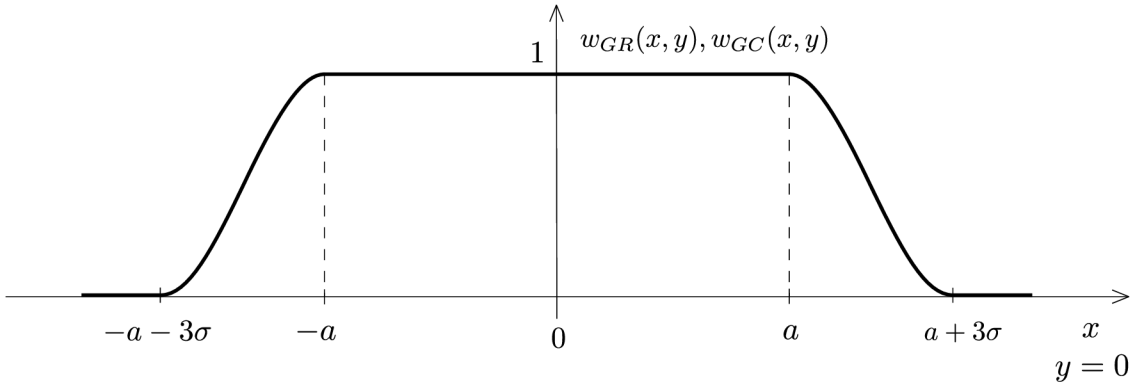


Figure 4.1: Graph of a $y = 0$ cut of function $w_{GR}(x, y), w_{GC}(x, y)$ for $r = a$, from [1]

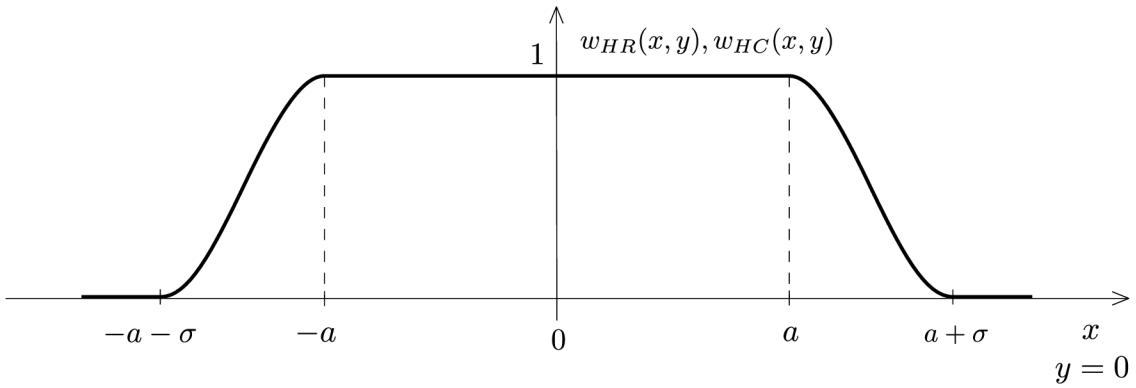


Figure 4.2: Graph of a $y = 0$ cut of function $w_{HR}(x, y), w_{HC}(x, y)$ for $r = a$, from [1]

We are using the Hanning window function in the implementation. That is due to the zero on the edges, which it creates. On the other hand, Gauss window function does not create zeros necessarily, it creates almost zeros, which are sufficient after all. However, it preserves smaller part of the image for the same $\sigma$ and has steeper decrease.

As we can see at Figures 4.1 and 4.2, the choice of set $A$ or $B$ together with appropriate $\sigma$ is significant. With wrong choice of the previously mentioned, we could end up with edges not even almost zero.

The rectangular window functions keep more information of the image. However, there is still some information about image edges. It is not necessary to apply the same image function to both images, in some cases it can be even preferable to use different image functions, depending on the distribution of structures in the image.

## 4.3 Low-pass weight function

The usage of low-pass together with high-pass weight functions is very good way to get rid of the influence of additive noise and variable impulse noise. They also reveal hardly visible structures in high dynamic range image. Noises are mainly represented

in the highest spatial frequencies of the image spectra, hardly visible structures (for example largest-scale structures such as optics vignetting and diffuse light in the optical system) are mainly represented in the lowest spatial frequencies of the images. We use the low-pass weight function to suppress the highest spatial frequencies of the image and the+high-pass weight function to suppress the lowest frequencies. The way of using these weight functions is to multiply the Fourier spectra by them.

However, the high-pass weight function is mentioned only for completeness, it is not used in the implementation. It might seem that it is not necessary to use the low-pass weight function too. In artificially made images, there is no additive or variable impulse noise. But as we can see in the program, the Gaussian low-pass weight function (see Definition 4.4) helps to bring up the peaks of the phase-correlation function and it helps with more precise computation of sub-pixel shifts too, as will be mentioned later.

**Definition 4.3. (Low-pass high-pass weight function)**[1] Let $r_1, r_2, \sigma_1, \sigma_2 \in \mathbb{R}^+$ such that $r1 < r_2$. Function $H_{r_1,\sigma_1}(\xi,\eta) : \mathbb{R}^2 \longrightarrow \langle 0,1\rangle$ defined as

$$H_{r_1,\sigma_1}(\xi,\eta) = \begin{cases} 0 & \text{if } \dfrac{4}{N^2}(\xi^2+\eta^2) < (r_1-\sigma_1)^2 \\ \dfrac{1}{2}\left(1+\cos\dfrac{\pi\left(r_1-\dfrac{2}{N}\sqrt{\xi^2+\eta^2}\right)}{\sigma_1}\right) & \text{if } (r_1-\sigma_1)^2 \le \dfrac{4}{N^2}(\xi^2+\eta^2) < r_1^2 \\ 1 & \text{else} \end{cases}$$

is called *high-pass weight function.* Function $H^{r_2,\sigma_2}(\xi,\eta) : \mathbb{R}^2 \longrightarrow \langle 0,1\rangle$ defined as

$$H^{r_2,\sigma_2}(\xi,\eta) = \begin{cases} 1 & \text{if } \dfrac{4}{N^2}(\xi^2+\eta^2) < r_2^2 \\ \dfrac{1}{2}\left(1+\cos\dfrac{\pi\left(r_2-\dfrac{2}{N}\sqrt{\xi^2+\eta^2}\right)}{\sigma_2}\right) & \text{if } r_2^2 \le \dfrac{4}{N^2}(\xi^2+\eta^2) < (r_2+\sigma_2)^2 \\ 0 & \text{else} \end{cases}$$

is called the *low-pass weight function.* Function $H^{r_2,\sigma_2}_{r_1,\sigma_1}(\xi,\eta) : \mathbb{R}^2 \longrightarrow \langle 0,1\rangle$ defined as

$$H^{r_2,\sigma_2}_{r_1,\sigma_1}(\xi,\eta) = H_{r_1,\sigma_1}(\xi,\eta)\cdot H^{r_2,\sigma_2}(\xi,\eta)$$

is called the *low-pass high-pass weight function.*

The low-pass high-pass function can be seen in Figure 4.3.

Further, we will consider only the low-pass weight function, because (as mentioned) we are using only it in the program. The alone low-pass weight function can be seen in Figure 4.4.

Like window function, the low-pass weight function is defined symmetrical with center $[0,0]$. Applied on images, it needs to be shifted by $(\frac{N}{2},\frac{N}{2})$, i.e. we multiply the Fourier spectra of the images by function $H^{r_2,\sigma_2}\left(\xi-\frac{N}{2},\eta-\frac{N}{2}\right)$.

It is possible to use different weight functions on each image. For instance, we can estimate different additive noises in images in some cases. However, choosing appropriate parameters is complicated and it is usually done manually.

In most cases, the computed shifts are not less precise, if we apply the low-pass function only once on the normalized cross-power spectrum of the images (the reason why it is

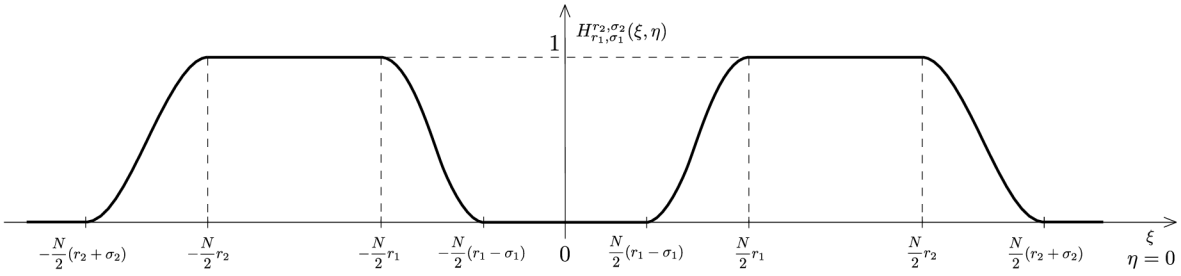


Figure 4.3: Graph of a $\eta = 0$ cut of function $H^{r_2,\sigma_2}_{r_1,\sigma_1}(\xi,\eta)$, shown in [1]

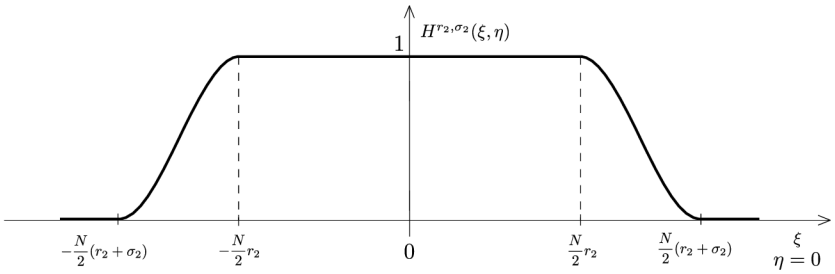


Figure 4.4: Graph of a $\eta = 0$ cut of function $H^{r_2,\sigma_2}(\xi,\eta)$

used the normalized spectrum will be explained later). It fastens the computations and it enables us to avoid dividing by zero. Then the formula for modified phase correlation is

$$\mathcal{D}^{-1}\left\{H^{r_2,\sigma_2}\left(\frac{F(\xi,\eta)\cdot G^*(\xi,\eta)}{|F(\xi,\eta)|\cdot|G(\xi,\eta)|}\right)\right\}$$

which remains real due to Corollary 3.25.

If there is no need to use low-pass function (as in our case with no additional noise in artificial created images), it can be replaced by the Gaussian low-pass weight function.

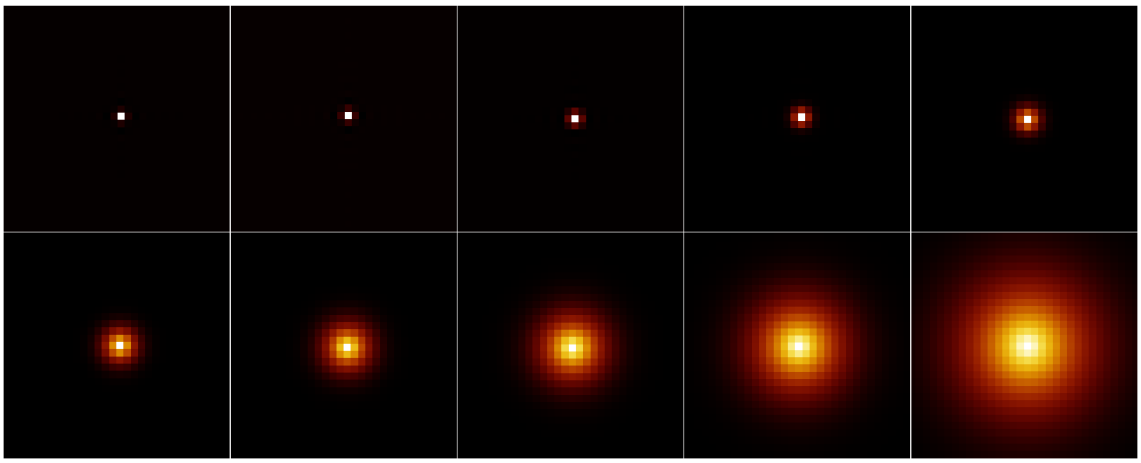

Figure 4.5: Details of peaks of the phase-correlation function (normalized autocorrelation function) with Gaussian low-pass weight function applied to the normalized cross-power spectrum, where $\lambda = 2, 4, 8, 16, ..., 1024$

**Definition 4.4. (Gaussian low-pass weight function)**[1] Let $\lambda \in \mathbb{R}_0^+$. Function $H_\lambda(\xi, \eta) : \mathbb{R}^2 \longrightarrow \langle 0, 1\rangle$ defined as

$$H_\lambda(\xi, \eta) = \mathrm{e}^{-\lambda \frac{\xi^2 + \eta^2}{N^2}}$$

is called the *Gaussian low-pass weight function* with parameter $\lambda$.

Influence of the $\lambda$ parameter of the Gaussian low-pass weight function is illustrated in Figure 4.5.

## 4.4 Finding shifts of shifted images

As said, we will find the shifts of shifted images at first. Let us summarize all the modifications and algorithms and after that, let us describe particular steps. The further described algorithm is the algorithm used in the program executed after uploading the input images (best in `*.bmp` format) and after clicking on button `Find translation only`. The method is taken from [1].

All the methods and procedures used to find shifts of shifted objects were developed by prof. Miloslav Druckmüller.

Let us denote $f, f_{sh}$ to be input images, which we are finding the shift of. For computing the Fourier transform, we will use a square $N \times N$ (where $N$ is an even number).

1. Multiplication of the images $f, f_{sh}$ by Hanning window function, obtaining images $f_w, f_{sh,w}$
2. Centering images $f_w, f_{sh,w}$ in the square $N \times N$ pixels, obtaining images $f_c, f_{sh,c}$
3. Computing the normalized cross-power spectrum $Z_{f_c,f_{sh,c}}$ of images $f_c, f_{sh,c}$
4. Multiplication of $Z_{f_c,f_{sh,c}}$ by Gaussian low-pass weight function, obtaining function $Z_w$
5. Computing the modified phase-correlation function as inverse discrete Fourier transform $P$ of $Z_w$
6. Finding the shift vector $(-x_0, -y_0)$ as the coordinates of the global maximum of function $P$ i.e. the coordinates $[x_0, y_0]$

By the choice of first applying the Hanning window function before the step 2, we are choosing to make the most of the image unchanged. We could swap the steps 1 and 2, but this way, we are keeping more information. In the program we can manually set the window function's parameters.

The normalized cross-power spectrum assures, that all the spatial frequencies are brought to consideration with same weight. There could occur problem with division by zero though. This problem appears in pixels with some of the spectra zero valued. It is treated in the program. When it comes to division by zero, there is no dividing at all and we consider just the cross-correlation spectrum value in this pixel. This does not lead to mistakes in finding shifts, because the value remains zero.

We also use the normalized cross-power spectrum to follow shifts of multiple objects in image, despite the fact that there is no theoretical justification as in case of finding

shift of shifted images. It does not bring as clear result as the Dirac impulse. But it is beneficial too, because it helps to get the peak in correlation function to be steeper, which leads to better recognition of similar shifts.

For the fourth step in the algorithm, we are choosing the $\lambda$ of the Gaussian low-pass weight function. The form of the parameter is $\lambda = 2^a$ and we are manually setting the $a$.

Step five is executed as defined in the Definition 3.5.

The output generated by the last step are the integer coordinates of the maximum valued pixel. The shift vector can be more precise (sub-pixel) by bringing to consideration even the neighbouring pixels. This will be more precisely described in following section.

It can happen that the shift vector is incorrect. It can be solvable by manual change of the low-pass weight function parameter.

## 4.5 Sub-pixel precision

This section derives from [1].

According to shape and values of the neighbourhood of the peak, there can be more precise estimation of the shift than only integer valued position of the global maximum.

We use the method based on geometric moments in the program. The sub-pixel precision estimate $(\bar{x_0}, \bar{y_0})$ of the shift vector is computed as

$$(\bar{x_0}, \bar{y_0}) = \left( \frac{M_{1,0}}{M_{0,1}}, \frac{M_{0,1}}{M_{0,1}} \right),$$

where $M_{k,l}$ is the geometric moment computed over a circle with center $[x_0, y_0]$ and radius $\varepsilon \in \mathbb{R}^+$, i.e.

$$M_{k,l} = \sum_{x^2+y^2<\varepsilon} \sum x^k y^l P(x_0 + x, y_0 + y), \qquad k, l = 0, 1,$$

where $P(x, y)$ is the modified phase correlation function computed in the algorithm in Section 4.4.

The parameter $\varepsilon$ needs to be manually set in the dependency on the size of the non-zero area around peak and its shape. The $\varepsilon$-area taken in consideration in the calculation is shown in the thumbnail.

## 4.6 Following of multiple objects movement

Theoretical results for Finding shifts of multiple objects in image are in Theorems 2.30, 2.31, 3.37 and 3.38. They all assume that objects are identical but shifted (as defined in Definitions 2.9 and 3.18).

So we are looking for local maxima in the modified phase correlation function computed by the algorithm introduced in Section 4.4. This part is more up to user than the previous parts. In the images with just one shift-vector, it is usually not so difficult to find the global maxima. In the case of Following of multiple objects movement, there could be a lot more incorrect results (i.e. local maxima which are not representing any shift vector, but for example the similarity of the objects). Thus, it is up to user to decide whether the result is the one which is wanted.

As is shown in the Theorems 3.35 and 3.36, the phase correlation function is periodic as result of periodicity or periodization of the input images in process. The peaks farther from the $[0, 0]$ are representing the periodized objects shifts. There are no obstacles

in Following of multiple objects movement, though. That is due to the fact, that the phase correlation function has lower values farther from the $[0, 0]$. In other words the local maxima close to the $[0, 0]$ have higher values than the ones farther.

This allows us to follow the multiple objects movement without high complexity of the computations. The first shift vector is found as global maxima of the phase correlation function (and with sub-pixel precision). The next shifts are found after transformation of the phase correlation function. The peak found in previous step must be deleted. That is performed by setting of the values of the peak and the pixels surrounding it to $\frac{1}{20}$ of the peak value. The size of the deleted surroundings is manually set by the user. The next shift is then found as the global maximum of the transformed phase correlation function.

The program used to implement the algorithm of Following multiple objects movement was developed by prof. Miloslav Druckmüller and then modified. All the adjustments were made in units `FFT` and `MainFormPhaseCorr`.

The algorithm is executed by clicking on button `Find multiple object translation` as follows:

Let us denote $f, g$ to be input images, which we are following the multiple objects movement in. For computing the Fourier transform, we will use a square $N \times N$ (where $N$ is an even number).

1. Multiplication of the images $f, g$ by Hanning window function, obtaining images $f_w, g_w$
2. Centering images $f_w, g_w$ in the square $N \times N$ pixels, obtaining images $f_c, g_c$
3. Computing the normalized cross-power spectrum $Z_{f_c,g_c}$ of images $f_c, g_c$
4. Multiplication of $Z_{f_c,g_c}$ by Gaussian low-pass weight function, obtaining function $Z_w$
5. Computing the modified phase-correlation function as inverse discrete Fourier transform $P_1$ of $Z_w$
6. Finding the shift vector $(-x_1, -y_1)$ as the coordinates of the global maximum of function $P_1$ i.e. the coordinates $[x_1, y_1]$
7. Finding the estimate of the sub-pixel shift vector by the geometrical moment method (see Section 4.5), obtaining estimate $(-\bar{x}_1, -\bar{y}_1)$
8. Deleting the peak $[x_1, y_1]$ together with its $\epsilon$ surroundings, if `Find next transformation` is executed, obtaining transformed function $P_2$
9. Finding the shift vector $(-x_2, -y_2)$ as the coordinates of the global maximum of function $P_2$ i.e. the coordinates $[x_2, y_2]$
10. Finding the estimate of the sub-pixel shift vector by the geometrical moment method, obtaining estimate $(-\bar{x}_2, -\bar{y}_2)$

We can repeat the steps 8.-10. after executing the `Find next transformation`, if we are not satisfied with the results or if we need to find next shift. All found shifts are recorded. The program can be seen in Figure 4.6.

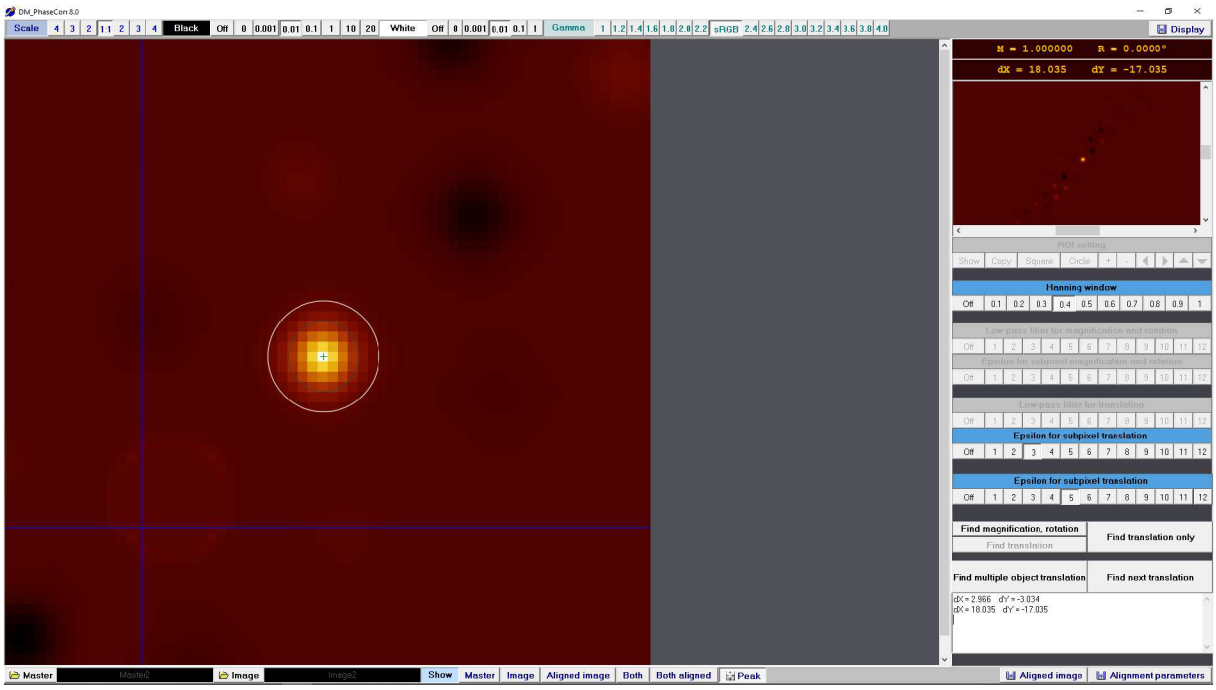


Figure 4.6: Program at work and with thumbnail after deleting the first global maximum

As mentioned above, it is possible to get the result which does not represent any of the shift vectors. In the Following of multiple objects movement, we can not revise it just by changing the low-pass weight function's parameter. It is due to the fact, that the phase correlation function needs to be recomputed after the parameter change. This would lead to restoration of all the deleted maxima. That would obviously compromise the process. Thus, while obtaining result, which is not representing any of the shift vectors, we are just looking for another shift, ignoring the incorrect result.

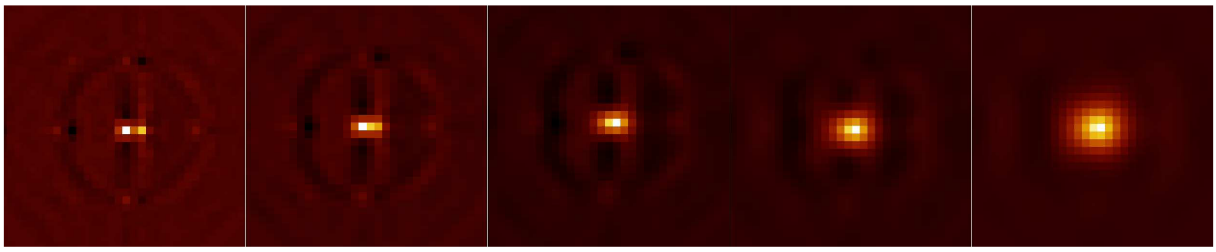

Figure 4.7: Illustration of incorrect shift search due to the similarity of the shift vectors. The shift vectors of the objects are $(17, 4; 3, 8)$ and $(20; 3, 8)$. Images illustrate the cuts of the phase correlation function with parameters of Gaussian low pass function equal to 4, 8, 16, 32, 64 (from the left). Clearly, the peaks of the last one are not distinguishable from each other

There are also restrictions on the form of image to proper work of the algorithm. As mentioned in the theoretical bases, the shift vectors need to be sufficiently different, or the peaks will merge and the algorithm can not distinguish them. On the other hand, if they are not sufficiently different and neither are almost the same, the shift vector of the almost merged peaks will be incorrect (it will be almost correct but not very precise). This is illustrated in Figure 4.7.

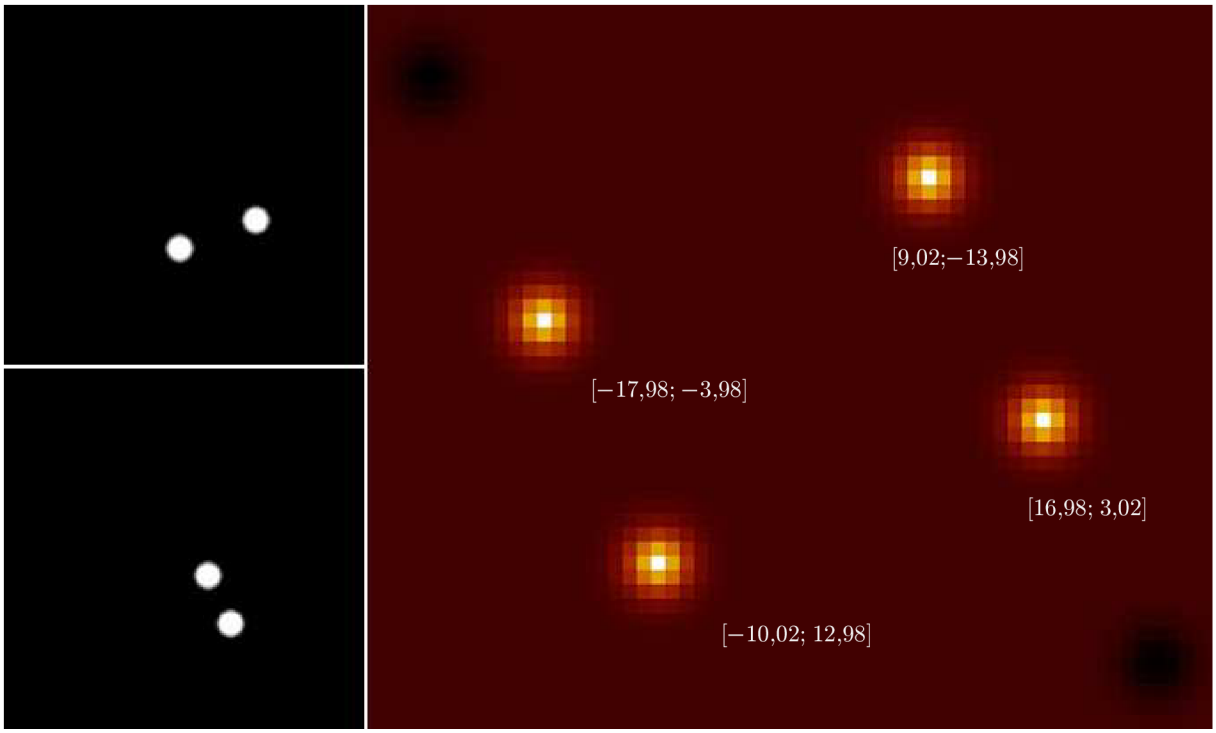


Figure 4.8: Illustration of incorrect shift search due to the similarity of the objects (they are same in this case). On the left are input images (master image on the top, image with shifted objects on the bottom) with shift vectors $(17,4;3,8)$ and $(-17,4;-3,8)$. The shifts are not clear, but from the found two shifts there have to be chosen the related ones

Other problem mentioned in the Theorem 2.30 may occur if some of the objects are similar or even same up to shift. This leads to creation of high local maxima as well. It is up to the user to judge which shifts are relevant in this case. This is illustrated in Figure 4.8.

There could also be another instance of incorrect shift search if the shift is too large. This means that if the shift of the object is greater than $\frac{\mu}{2}$ or $\frac{\nu}{2}$ in dependence of relevant axis, i.e. if the shift is greater than the half of the size of image $f$. Due to the periodicity of the function and due to the fact, that the maxima closer to $[0,0]$ are greater than the farther ones, there would be found a local maxima which is not linked to any shift. It is again up to user to decide, whether the found shift is relevant or not. This can be seen in Figure 4.9.

Due to the above mentioned problems and needs of user's judgement, it is clear that the process of Following the multiple objects movement by means of cross correlation can not be automatized.

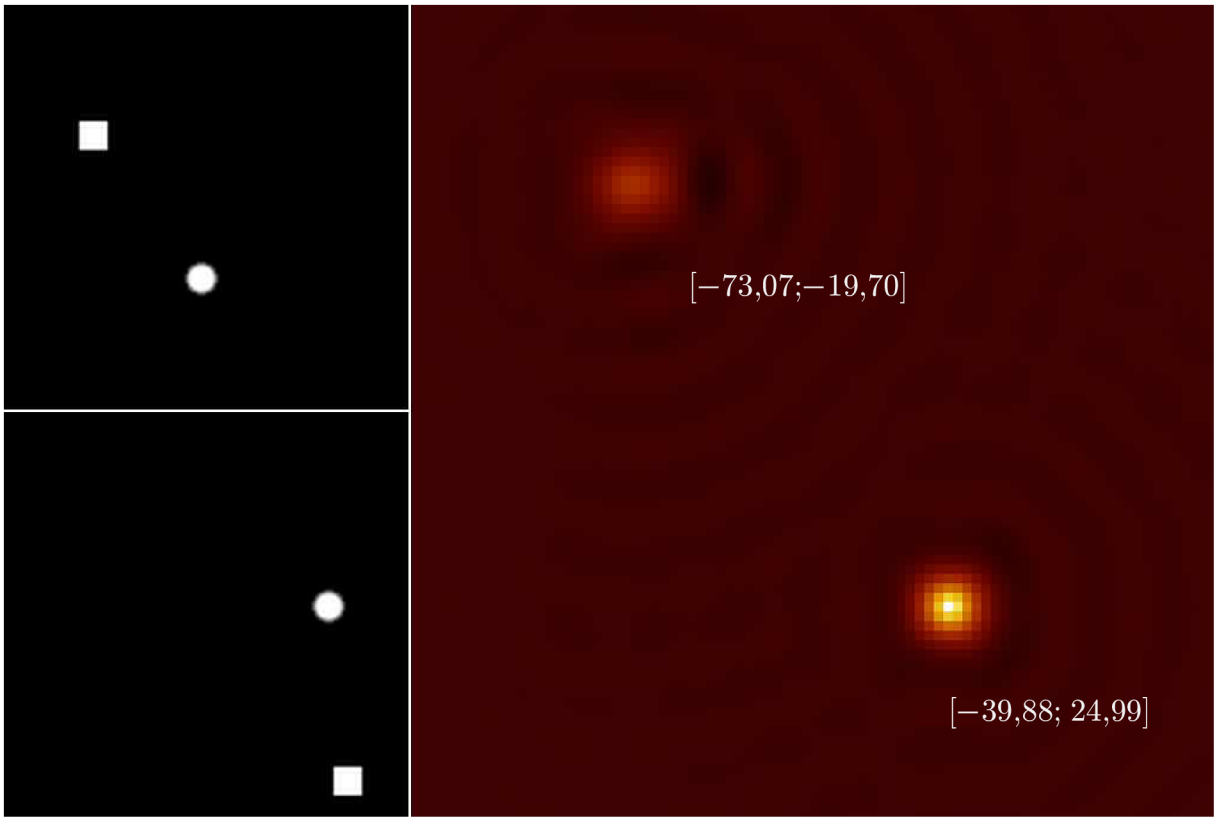


Figure 4.9: Illustration of incorrect shift search due to the too large shift. On the left are input images (master image on the top, image with shifted objects on the bottom), the size of the images is $128 \times 128$ and shift vectors of the shifted objects are $(39,8;-25,6)$ and $(80;75)$. The lower peak clearly does not correspond to any of the shift vectors. Neither there is peak representing the second shift vector in next found coordinates in this case

### 4.6.1 Testing precision on simulated data

The testing of the precision of implementation was executed on more the 30 artificially made testing images. For the simplification of the image creation, the original objects are white shapes on the black background. They were individually shifted by predefined shifts into all combinations of basic directions. The sub-pixel shifts were realized on the first decimals and by means of bilinear interpolation. The shifted objects were summed as defined in the Definitions 2.8, 3.17 with particular emphasis on them not to overlap and by the rules for the algorithm best to work as mentioned above. Most of the images consist of two objects however, there are also images with only one object or with three objects.

All the testing images are square with size $N = 128$ and they are enclosed on the CD. There is one master image (reference image, which are all the shifts related to) named `C_0_0__S_0_0__T_0_0.bmp` or just with part of the name. The letter represents the shape (`C` for circle, `S` for square, `T` for triangle), first number attached to letter represents the shift in $x$ axis, the second number in $y$ axis. There are another images with shifted objects with known shifts described in their names as explained.

The testing was executed with sub-pixel method mentioned in the Section 4.5. The best estimations of the first shifts were performed by individual choices of low-pass weight func-

tion's parameter and $\varepsilon$-surroundings to best fit the known shifts.

However, the next shifts search can be affected only by the choice of the $\varepsilon$-surroundings.

On the contrary to the Finding the shifts of shifted image (which can be performed precise up to the third decimal), the Following of multiple objects movement is precise only to the whole pixels. There were deviations up to $0,8$ in all directions and even in coordinates of the first peak, which could not be improved even by altering of both mentioned parameters.

# Chapter 5

# Conclusion

The main goal of this thesis was to describe the method of Following the multiple objects movement by means of cross correlation, to generalize it for two and more objects and to implement it.

The second chapter introduces the continuous Fourier transform and the inverse Fourier transform. There are presented the concepts of the shifted functions, the objects in the function and the function with shifted objects. There is also shown the impact of the Fourier transform applied to the shifted functions and the function with shifted objects considering the original functions. The convolution and the concept of cross correlation are also introduced in this chapter. We are introducing the cross-correlation function of shifted function in order to find their shift. Then we generalize it for two and more objects and show, that it can be used to follow the multiple objects movement. The second chapter serves to basically define all the notions mentioned above by means of the Functional analysis.

The third chapter presents all concepts of the first chapter in the discrete case. It is necessary to work with digital images, which are the discrete analogy of continuous function. There is also presented the periodization of the function essential for work with shifted images. We are introducing the cross-correlation function of shifted images in discrete case as well. There is also proven, that the discrete cross-correlation function of functions with shifted objects can be used to find their shifts. Which is the theoretical base for further implementation.

The fourth chapter describes the implementation of the aforesaid principles. At first, we are introducing the algorithm of Finding shifts of shifted images. The form of the input images is pointed out, especially their size and the window function and low-pass weight function, which have to be applied to the images. Furthermore, we are introducing the algorithm of Finding shifts of shifted images. This algorithm leads to the algorithm of Following the multiple objects movement directly. There are also shown the problems connected to the algorithm, primarily including the form of input images. Thus, we justify the statement, that the process of following of multiple objects movement by means of cross correlation can not be automatized. Lastly, we are testing the precision of the algorithm and finding out, that it computes with precision in whole pixels on the artificial made images. That is the degradation of the precision performed by the algorithm of Finding the shifts of the shifted images.

# Bibliography


[1] DRUCKMÜLLEROVÁ, Hana. *Phase-correlation based image registration.* Brno, 2010. Master's thesis, Fakulta strojního inženýrství Vysoké učení technické v Brně.

[2] NOVÝ, J. *Digital filtering and compression in image processing and volume rendering.* Brno, 2005. PhD thesis. Brno University of Technology, Faculty of Mechanical Engeneering. Vedoucí práce Druckmüller, M.

[3] DRUCKMÜLLER, Miloš. Phase correlation method for the alignment of total solar eclipse images. *The Astrophysical Journal.* 706. 2009, (2), 1605-1608. ISSN 0004-637X.

[4] ČÍŽEK, Václav. *Diskretní Fourierova transformace a její použití.* Praha: SNTL - Nakladatelství technické literatury, 1981. Matematický seminář SNTL, sv. 16.

[5] KOMRSKA, Jiří. *Fourierovské metody v teorii difrakce a ve strukturní analýze: texty přednesené na FSI VUT v Brně studentům 3. ročníku oboru "Fyzikální inženýrství" , 4. ročníku oboru "Přesná mechanika a optika" a doktorandům v roce 2000.* Brno: VUTIUM, 2001. ISBN 80-214-2011-1.

[6] STEIN, Elias M. a Guido WEISS. *Introduction to Fourier analysis on Euclidean spaces.* Princeton, N.J.: Princeton University Press, 1971. ISBN 0-691-08078-x.

[7] FOLLAND, G. B. *Fourier analysis and its applications.* Providence, R.I.: American Mathematical Society, 2009. Sally series (Providence, R.I.), 4. ISBN 0821847902.

[8] BEZVODA, Václav. *Dvojrozměrná diskrétní Fourierova transformace a její použití.* Praha: Státní pedagogické nakladatelství, 1988.

[9] FRANCŮ, Jan. *Moderní metody řešení diferenciálních rovnic.* Vyd. 2., rozš. Brno: Akademické nakladatelství CERM, 2006. ISBN 80-214-3329-9.

[10] *Stack.exchange.com* [online]. [cit. 2019-05-23]. Dostupné z: `https://dsp.stackexchange.com/questions/31240/how-to-prove-that-the-peak-of-the-autocorrelation-function-is-at-zero-lag`

# Used symbols

| | |
|---|---|
| $\mathbb{N}$ | the set of natural numbers |
| $\mathbb{Z}$ | the set of integer numbers |
| $\mathbb{R}$ | the set of real numbers |
| $\mathbb{C}$ | the set of complex numbers |
| $\mathcal{L}(\mathbb{R}^2)$ | space of all functions $\mathbb{R}^2 \longrightarrow \mathbb{C}$ with finite integral of $\lvert f \rvert$ |
| $C^1$ | class of continuous functions with continuous derivatives |
| $a^*$ | the complex conjugate of $a \in \mathbb{C}$ |
| $\lfloor a \rfloor$ | the integral part of real number $a$ |
| $\mathcal{F}$ | the Fourier transform, see Definition 2.3 |
| $\mathcal{F}^{-1}$ | the inverse Fourier transform, see Definition 2.4 |
| $\mathcal{D}$ | the discrete Fourier transform, see Definition 3.4 |
| $\mathcal{D}^{-1}$ | the inverse discrete Fourier transform, see Definition 3.5 |
| $f(x,y), g(x,y)$ | functions from $\mathcal{L}(\mathbb{R}^2)$ or functions $\{0,1,...,N-1\}^2 \longrightarrow \mathbb{R}$, $N \in \mathbb{N}$ |
| $N$ | size of the domain of functions defined on $\{0,1,...,N-1\}^2 \longrightarrow \mathbb{R}, N \in \mathbb{N}$, $N$ is supposed to be even number |
| $f_i(x,y)$ | objects of the functions, see Definitions 2.8,3.17 |
| $n$ | number of objects in the function, see Definitions 2.8,3.17 |
| $f_{sh}, f_{i,sh}$ | shifted functions of functions $f, f_i$, see Definitions 2.6,3.13 |
| $F(\xi,\eta), G(\xi,\eta)$ | the Fourier spectra of functions $f(x,y), g(x,y)$, see Definitions 2.3, 3.4 |
| $F_i(\xi,\eta)$ | the Fourier spectra of objects $f_i$ |
| $F_{sh}(\xi,\eta), F_{i,sh}(\xi,\eta)$ | the Fourier spectra of shifted functions $f_{sh}, f_{i,sh}$ |
| $(x_i, y_i)$ | the shift vector of object $f_{i,sh}$, or shift vector of shifted function $f_{sh}$, see Definitions 2.6, 3.13, 2.9, 3.18 |
| $f * g$ | the convolution of functions $f, g$, see Definitions 2.19, 3.26 |
| $\tilde{f}, \tilde{g}, \tilde{f_i}$ | the periodization of functions $f, g, f_i$, see Definition 3.7 |
| $C_{f,g}(\xi,\eta)$ | the cross-power spectrum of functions $f, g$, see Definitions 2.24, 3.30 |
| $Z_{f,g}(\xi,\eta)$ | the normalized cross-power spectrum of functions $f, g$, see Definitions 2.24, 3.30 |
| $Q_{f,g}(x,y)$ | the cross-correlation function of functions $f, g$, see Definitions 2.25, 3.31 |
| $P_{f,g}(x,y)$ | the phase correlation function of functions $f, g$, see Definitions 2.25, 3.31 |
| $\delta(x,y)$ | the Dirac distribution, see Definition 2.2 |
| $d(x,y)$ | the discrete impulse function, see Definition 3.34 |
| $\mu, \nu$ | the width and height of the input image, see Section 4.1 |
| $w_{GR}, w_{GC}, w_{HR}, w_{HC}$ | Gaussian and Hanning, rectangular and singular window |

| | |
|---|---|
| | functions, see Definitions 4.2, 4.1 |
| $\lambda$ | the parameter of Gaussian low-pass weight function, see Definition 4.4 |
| $f_c, g_c, f_{sh,c}$ | the centred input images surrounded by black area, see Section 4.1 |
| $(\bar{x}_i, \bar{y}_i)$ | the sub-pixel estimation of shift vector, see Section 4.5 |
| $\varepsilon$ | the radius of the surroundings of the peak in sub-pixel peak search, see Section 4.5 |
| $\epsilon$ | the radius of deleted surroundings of the peak, see Section 4.6 |

# Appendix

CD with program in Delphi 7 and with testing images in `*.bmp`.